USING THE ELECTRICAL ACTIVITY OF THE DIAPHRAGM TO DETERMINE THE WORK OF BREATHING IN INFANTS ON HIGH FLOW NASAL CANNULA THERAPY

Trang Minh Thi PHAM, BEng (Electrical and Computer)

Submitted in fulfilment of the requirement for the degree of

BN72 Master of Engineering (Research)

School of Electrical Engineering and Computer Systems
Faculty of Science and Engineering
Queensland University of Technology

2016

KEYWORDS

Electrical Activity of the Diaphragm
Neurally Adjusted Ventilatory Assist
Non-Invasive Ventilation
High Flow Nasal Cannula
Work of Breathing
Oesophageal Pressure
Pressure-Rate Product
Pressure-Time Product
Thoraco-Abdominal Asynchrony
Respiratory Inductance Plethysmography
Lissajous Loop Analysis
Electrical Impedance Tomography
Bronchiolitis
Paediatric Intensive Care

ABSTRACT

The physiological effect of high flow nasal cannula (HFNC) therapy is presumed to be a decrease in work of breathing (WOB) through an offloading of the diaphragm during inspiration with an increased expiratory resistance and accompanying positive end-expiratory pressure (PEEP) during expiration. To determine whether this can be assessed objectively using a signal of the electrical activity of the diaphragm, measurements were taken off and then on HFNC, delivered at 2L/kg/min, in infants with (Bronchiolitis) and without (Cardiac) obstructive airways disease, and compared with other traditional measures of WOB.

The electrical activity of the diaphragm (Edi) was measured using an Edi catheter and analysed for determinants of respiratory drive (signal peak Edi_{MAX} and amplitude Edi_{AMPL}). Respiratory Inductance Plethysmography (RIP) was analysed for changes in end-expiratory lung volume (RIP_{MIN}) and a phase angle (θ) of thoraco-abdominal asynchrony (TAA), calculated using the Lissajous Loop Analysis (LLA) method. Traditional WOB measurements, Pressure-Rate Product (PRP) and Pressure-Time Product (PTP) were calculated from analyses of oesophageal pressure (Poe).

While the electrical activity of the diaphragm was higher in infants with Bronchiolitis than in Cardiac infants, significant decreases in respiratory drive (Edi_{MAX}, Edi_{AMPL}) were observed in both groups ($p<0.05$). Infants with Bronchiolitis showed a significant increase in RIP_{MIN} ($p<0.05$), while Cardiac infants showed a decrease in θ ($p<0.05$). WOB decreased in both groups with a significant reduction of PRP and PTP ($p<0.05$).

HFNC therapy, delivered at 2L/kg/min, offloads the diaphragm and is highly effective in reducing WOB in infants with Bronchiolitis. Measurements of the electrical activity of the diaphragm provide a useful clinical tool for the objective assessment of WOB. Changes in the electrical activity of the diaphragm are a more sensitive measure for detecting WOB changes compared with traditional measures of WOB.

TABLE OF CONTENTS

KEYWORDS 2
ABSTRACT 3
TABLE OF CONTENTS 4
LIST OF FIGURES 7
LIST OF TABLES 10
LIST OF ABBREVIATIONS 11
STATEMENT OF ORIGINAL AUTHORSHIP 14
ACKNOWLEDGEMENT LIST 15
1 INTRODUCTION 16
1.1 Background 16
1.2 Context 17
1.3 Purposes 18
1.4 Significance 18
1.5 Thesis Outline 19
2 LITERATURE REVIEW 20
2.1 NAVA and the Electrical Activity of the Diaphragm 20
2.2 Mechanisms of Action of HFNC 21
2.3 Determining the Work of Breathing 23
3 METHODS 26
3.1 Materials and Measurements 27
3.1.1 HFNC Device 27
3.1.2 Electrical Activity of the Diaphragm 28
3.1.3 Respiratory Inductance Plethysmography 29
3.1.4 Oesophagus Pressures 29
3.1.5 Electrical Impedance Tomography 30
3.1.6 Data Acquisition using PowerLab 30
3.2 Measurement Analysis 31
3.2.1 Edi, RIP_{SUM} and Poe 31
3.2.2 Traditional WOB Calculations 31
3.2.3 Lissajous Loop Analysis 32
3.2.4 EIT 33

3.3 Implementation in LabChart 34
3.4 Statistics 34
4 RESULTS 35
4.1 Electrical Activity of the Diaphragm 35
4.2 Respiratory Inductance Plethysmography 37
4.3 Oesophagus Pressure 39
4.4 Lissajous Loop Analysis 41
4.5 Electrical Impedance Tomography 45
4.6 Publications 47
5 DISCUSSION 48
5.1 WOB Measurements and Assessments 48
5.1.1 Electrical Activity of the Diaphragm 48
5.1.2 Respiratory Inductance Plethysmography 48
5.1.3 Oesophageal Pressure 49
5.1.4 LLA for TAA 49
5.2 WOB Measures for HFNC 50
5.2.1 Clinical Significance of Research Findings 50
5.2.2 Future Directions for WOB and HFNC Flow Rate Titration 51
5.3 Limitations 52
5.4 Conclusion 53
APPENDICES 54
A.1 Background to Methodology 54
A.1.1 The Clinical High Flow Work of Breathing Study 54
A.1.2 Study Design 55
A.1.3 Timeline for Completion 55
A.2 LabChart Analysis 56
A.2.1 Design Limitations and Restrictions 56
A.2.2 Macro Sequences 57
A.2.3 Example LabChart Waveform Recordings 59
A.2.4 Example LabChart Macro Recordings 62
A.3 EIT Results using the EIT Data Analyser 66
A.4 Clinical Findings 69
A.4.1 The Clinical HFWOB Study 69
A.4.2 Clinical WOB Scoring: Results 69

A.4.3 Clinical WOB Scoring: Discussion 71
REFERENCES 72

LIST OF FIGURES

Figure 1: Conceptualised equipment set-up and connection diagram for the broader clinical study from which this program of research is based.

Figure 2: An illustration of the standard High Flow Nasal Cannula system, used in the broader clinical study from which this program of research is based, manufactured by Fisher & Paykel Healthcare.

Figure 3: An illustration of the Edi monitoring function of a Servo-i ventilator, manufactured by MAQUET, which was used in isolation to monitor the Edi signal of patients receiving High Flow Nasal Cannula therapy.

Figure 4: An illustration of the placement of disposable bands used in the measurement of Respiratory Inductance Plethysmography.

Figure 5: An illustration of the ECG electrode placement used in the measurement of Electrical Impedance Tomography.

Figure 6: Representative overall inspiratory RIP_{SUM} and oesophageal pressure (Poe) waveforms with a signal showing the start of inspiration. Includes brief descriptions of calculations based on the RIP_{SUM} and Poe signals.

Figure 7: The phase angle of TAA is calculated from the equation $\sin \theta = m/s$, where m is the distance traversed by the ABD at the mid-point of the RC excursion and s is the overall ABD excursion.

Figure 8: Representative recording of the electrical activity of the diaphragm showing the effect of removing and reapplying HFNC therapy.

Figure 9: Mean values of the electrical activity of the diaphragm for infants with Bronchiolitis and Cardiac infants, off and on HFNC.

Figure 10: Mean values of the overall Respiratory Inductance Plethysmography waveform (RIP_{SUM}) for infants with Bronchiolitis and Cardiac infants, off and on HFNC.

Figure 11: Mean values in the Oesophageal Pressure waveform and related WOB calculations for infants with Bronchiolitis and Cardiac infants, off and on HFNC.

Figure 12: Representative Lissajous Loops of the rib cage and abdomen signals on an X-Y plot, taken from Respiratory Inductance Plethysmography recordings, for an infant with Bronchiolitis and a Cardiac infant, off and on HFNC.

Figure 13: Mean values of the Lissajous Loop Analysis related calculations for infants with Bronchiolitis and Cardiac infants, off and on HFNC.

Figure 14: Representative Electrical Impedance Tomography recordings showing the effect of removing and reapplying HFNC therapy.

Figure 15: Representative Electrical Impedance Tomography images showing ventilation distribution (a) off HFNC and (b) on HFNC therapy.

Figure 16: Representative LabChart recording of the RC, ABD, RIP_{SUM} and Edi signals of an infant on HFNC delivered at 2L/kg/min.

Figure 17: Representative LabChart recording of the RC, ABD, RIP_{SUM} and Poe signals of an infant on HFNC delivered at 2L/kg/min.

Figure 18: Representative example of synchronised pre-processed EIT signals inserted in to a LabChart file.

Figure 19: Representative result waveforms from the first LabChart Macro (Macro I: Edi and RIP_{SUM} Analysis).

Figure 20: Representative result waveforms from the second LabChart Macro (Macro II: LLA Analysis).

Figure 21: Representative result waveforms from the third LabChart Macro (Macro III: EIT, Poe and RIP_{SUM} Analysis).

Figure 22: Representative result waveforms from the fourth LabChart Macro (Macro IV: RIP_{SUM}, Poe, PRP, PTP(di) and PEEPi Analysis).

Figure 23: Mean values of the Electrical Impedance Tomography calculations for infants with Bronchiolitis and Cardiac infants, off and on HFNC.

Figure 24: Individual WOB category assessments for infants with Bronchiolitis and Cardiac infants, off and on HFNC.

Figure 25: Observed values of respiratory rate and oxygen saturation, used in the clinical scoring method of assessing WOB and respiratory distress, for infants with Bronchiolitis and Cardiac infants, off and on HFNC.

LIST OF TABLES

Table 1: Mean values and absolute mean changes of the electrical activity of the diaphragm for infants with Bronchiolitis and Cardiac infants, off and on HFNC.

Table 2: Mean values and absolute mean changes in the Respiratory Inductance Plethysmography measurements taken for infants with Bronchiolitis and Cardiac infants, off and on HFNC.

Table 3: Mean values and absolute mean changes of the oesophageal pressure calculations for infants with Bronchiolitis and Cardiac infants, off and on HFNC.

Table 4: Mean values and absolute mean changes of the Lissajous Loop Analysis related calculations for infants with Bronchiolitis and Cardiac infants, off and on HFNC.

Table 5: Mean values and absolute mean changes in the pre-processed Electrical Impedance Tomography waveforms for infants with Bronchiolitis and Cardiac infants, off and on HFNC.

Table 6: Mean values and absolute mean changes in the Electrical Impedance Tomography measurements taken for infants with Bronchiolitis and Cardiac infants, off and on HFNC. These results were obtained using the PCCRG's standardised EIT data analysis protocol (originally written by me) where calculations were performed separately from the main LabChart analysis.

Table 7: Respiratory assessment guidelines, as used by clinical staff at the MCH PICU, include observable WOB criteria. Standard assessments are objective and based on the clinical experience of the observer.

LIST OF ABBREVIATIONS

A_{AMPL}	Anterior amplitude
ABD	Abdomen
ABD_{AMPL}	ABD amplitude
ABD_{MAX}	ABD maxima
ABD_{MIN}	ABD minima
A_{MAX}	Anterior maxima
A_{MIN}	Anterior minima
AUC	Area under the curve
BNC	Bayonet Neill–Concelman
CHD	Congenital Heart Disease
CI	Confidence Interval
CMV	Conventional Mechanical Ventilation
CO_2	Carbon Dioxide
CPAP	Continuous Positive Airway Pressure
ECG	Electrocardiography
Edi	Electrical Activity of the Diaphragm
Edi_{AMPL}	Edi amplitude
Edi_{AUC}	Edi area under the curve
Edi_{MAX}	Inspiratory maximum Edi
Edi_{MIN}	End-expiratory level Edi
Edi_{RR}	Respiratory rate Edi
EEL	End-Expiratory Level
EELV	End-Expiratory Lung Volume
EIT	Electrical Impedance Tomography
$EIT_{ANTERIOR}$	Anterior region of the lungs, as measured by EIT
EIT_{GLOBAL}	Overall respiratory movement, as measured by EIT
$EIT_{POSTERIOR}$	Posterior region of the lungs, as measured by EIT
FI	Filling Index
FiO_2	Fraction of inspired oxygen
G_{AMPL}	Global amplitude
GC	Geometric Centre of ventilation

GI	Global Inhomogeneity index
G_{MAX}	Global maxima
G_{MIN}	Global minima
HFNC	High Flow Nasal Cannula
HFWOB	Clinical High Flow Work of Breathing Study
HREC	Human Research Ethics Committee
INV	Invasive Ventilation
L/kg/min	Litres per kilogram per minute
LAA	Lissajous Loop Analysis
m	Distance traversed by the ABD at the mid-point of the overall RC excursion, in a Lissajous Loop diagram
MCH	Mater Children's Hospital
MHS	Mater Health Services
MRI-UQ	Mater Research Institute – The University of Queensland
NAVA	Neurally Adjusted Ventilatory Assist
NG	Nasogastric tube
NIV	Non-Invasive Ventilation
NIV-NAVA	Non-Invasive Neurally Adjusted Ventilatory Assist
O_2	Oxygen
P_{AMPL}	Posterior amplitude
PCCRG	Paediatric Critical Care Research Group
PEEP	Positive End-Expiratory Pressure
PEEPi	Intrinsic Positive End-Expiratory Pressure
PICU	Paediatric Intensive Care Unit
P_{MAX}	Posterior maxima
P_{MIN}	Posterior minima
Poe	Oesophageal Pressure
Poe_{AMPL}	Poe amplitude
$\int Poe_{INSP}$	Integral of the Poe curve during inspiration
Poe_{MAX}	Maximum respiratory Poe point
Poe_{MIN}	Minimum respiratory Poe point
PRP	Pressure-Rate Product
PTI	Pressure-Time Index
PTP	Pressure-Time Product

PTP(di)	Diaphragmatic Pressure-Time Product
PTP(mod)	Modified Pressure-Time Product
QUT	Queensland University of Technology
RC	Rib Cage
RC_{AMPL}	RC amplitude
RC_{MAX}	RC maxima
RC_{MIN}	RC minima
RIP	Respiratory Inductance Plethysmography
RIP_{ABD}	Abdominal excursions, as measured by RIP
RIP_{AMPL}	Amplitude of tidal breathing, as measured by RIP
RIP_{AUC}	Area under the curve, as measured by RIP
RIP_{MAX}	Inspiratory peak, as measured by RIP
RIP_{MIN}, RIP_{EEL}	End-expiratory level, as measured by RIP
RIP_{RC}	Rib cage excursions, as measured by RIP
RIP_{RR}	Respiratory rate, as measured by RIP
RIP_{SUM}	Overall respiratory movement, as measured by RIP
RIP_{Ti}	Inspiratory time to peak, as measured by RIP
$RIP_{Ti/Ttot}$	The ratio between the inspiratory-phase to length of entire respiratory cycle
RIP_{Ttot}	Respiratory cycle length, as measured by RIP
RR	Respiratory Rate
RSV	Respiratory Syncytial Virus
s	Overall ABD excursion, in a Lissajous Loop diagram
SaO_2	Arterial Oxygen Saturation
SpO_2	Peripheral oxygen saturation
SUM	Overall respiratory movement signal, as measured by RIP
TAA	Thoraco-Abdominal Asynchrony
UQ	The University of Queensland
VBA	Visual Basic for Applications
V_T	Tidal Volume
WOB	Work of Breathing
θ	Phase Angle of TAA

STATEMENT OF ORIGINAL AUTHORSHIP

The work contained in this thesis has not been previously submitted to meet requirements for an award at this or any other higher education institution. To the best of my knowledge and belief, the thesis contains no material previously published or written by another person except where due reference is made.

Signature: QUT Verified Signature

Date: September 2016

ACKNOWLEDGEMENT LIST

A/Prof Bouchra Senadji (Principal Supervisor), QUT

Prof Vinod Chandran (Associate Supervisor), QUT

Mr Kimble Dunster (former Associate Supervisor), QUT

Dr Ed Palmer (former Principal Supervisor), QUT

Associate Professor Andreas Schibler, MRI-UQ

Ms Sara Mayfield, MRI-UQ

Ms Lee O'Malley, MRI-UQ

Ms Jacqueline Jauncey-Cooke, UQ

Paediatric Critical Care Research Group, MRI-UQ

Paediatric Intensive Care Unit, MCH

1 INTRODUCTION

This program of research forms part of a broader clinical study, investigating the impact of high flow nasal therapy on the work of breathing in infants with bronchiolitis, which was conducted by the Paediatric Critical Care Research Group (PCCRG), in the Paediatric Intensive Care Unit (PICU) of the Mater Children's Hospital (MCH). This chapter outlines the background of this broader clinical study to highlight the context, objectives and significance of this program of research. A brief outline of the remaining chapters of this thesis is also provided.

1.1 Background

Bronchiolitis, with an underlying viral infection, is the most common cause of hospitalisation among infants in the first 12 months of life (Castro-Rodriguez, Rodriguez-Martinez et al. 2015) and remains one of the main reasons for non-elective admissions to paediatric intensive care (Alexander, Millar et al. 2014). Bronchiolitis is characterised by acute inflammation, oedema, and necrosis of the epithelial cells lining the small airways, and increased mucus production (Ralston, Lieberthal et al. 2014). Among available treatment options, non-invasive oxygen supplementation remains the mainstay of therapy (Ravaglia and Poletti 2014) (Da Dalt, Bressan et al. 2013). Oxygen therapy, administered via a heated humidified high flow nasal cannula (HFNC) is a recently introduced form of non-invasive respiratory support (Spoletini, Alotaibi et al. 2015) (Mayfield, Jauncey-Cooke et al. 2014). The use of HFNC is increasing across a range of patient groups, due to its ease of application, patient tolerance and observed clinical benefits (Hutchings, Hilliard et al. 2015) (Nishimura 2015) (Mayfield, Jauncey-Cooke et al. 2013) (McQueen, Rojas et al. 2014) (Milési, Boubal et al. 2014) (Manley, Dold et al. 2012). In intensive care, retrospective studies have shown that HFNC can be applied safely and effectively, reducing intubation rates, in children less than two years of age with bronchiolitis (Schibler, Pham et al. 2011) (McKiernan, Chua et al. 2010) . However, despite the increasing use of HFNC therapy in the treatment of infants with Bronchiolitis (Da Dalt, Bressan et al. 2013) (Hutchings, Hilliard et al. 2015), the predominant mechanism of action of HFNC is not well established (Dysart, Miller et al. 2009). Previous studies have investigated the postulated mechanisms of action of HFNC in relation to positive pressure generation (Sinha, McBride et al. 2015) (Spoletini, Alotaibi et al. 2015), often in comparison with other non-invasive ventilation devices (Wilkinson, Andersen et al. 2016) (Kotecha, Adappa et al. 2015) (Lavizzari, Veneroni et al. 2014) (de Jongh, Locke et al. 2014),

but its impact on the work and breathing pattern of infants with Bronchiolitis remains unclear (Rubin, Ghuman et al. 2014) (Lee, Rehder et al. 2013).

1.2 Context

Since interventions to improve patient outcomes are dependent on available assessment methods, it is desirable to have an economical and minimally invasive or non-invasive method for assessing the work of breathing (WOB) in infants and children admitted to intensive care. Previously, WOB has been described in terms of the body's oxygen cost of breathing of the muscles involved in respiration (Collett, Perry et al. 1985), measured in Joules/Litre (Diehl, Mercat et al. 2003) or mL O_2/minute (Jones, Dean et al. 2003). However, methods for determining metabolic consumption are difficult and unsuitable in an intensive care setting (Collett and Engel 1986) (Cala, Wilcox et al. 1991). In the absence of robust measurement techniques, the determination of respiratory distress includes indicators for WOB and is commonly assessed with clinical scoring systems which are subjective and based on the clinical experience of the observer (Brochard, Martin et al. 2012) (Fallot 2005) (Rödl, Resch et al. 2012) (Gemke, van Keulen et al. 2005). Traditional methods, such as Lissajous Loop Analysis (LLA) calculations for the measurement of Thoraco-Abdominal Asynchrony (TAA), can be used as an indication of respiratory distress (Hammer and Eber 2005), and derived calculations, such as the Pressure-Rate Product (PRP), can be used as surrogate measures of WOB (Collett, Perry et al. 1985). However, these techniques do not measure WOB directly and are susceptible to disturbances from the measurement environment. Measurements of the electrical activity of the diaphragm (Edi) provide a more direct method for determining WOB and response to treatment from individual patients (Bellani, Mauri et al. 2013) (Ducharme-Crevier, Du Pont-Thibodeau et al. 2013).

The Edi signal, a signal arising from the diaphragm's neural activation during spontaneous breathing, is a validated measure of global respiratory drive (Sinderby, Beck et al. 1998) (Beck, Sinderby et al. 1998) and is currently used in mechanical ventilation systems to deliver respiratory support in both invasive (INV) and non-invasive ventilation (NIV) modes (Beck, Emeriaud et al. 2015). Neurally adjusted ventilatory assist (NAVA) is a new mode of closed-loop mechanical ventilation which delivers airway pressure in proportion to the Edi signal (Ververidis, Van Gils et al. 2011). As with other closed-loop controlled mechanical ventilation systems, ventilator variables required for the delivery of ventilator-triggered mandatory breaths, are automatically manipulated based on the continuous measurement of respiratory parameters from the patient (Suarez-Sipmann 2014). However,

these closed-loop ventilatory modes still require clinicians to specify individualised pressure limits, volume targets and proportionality constants to deliver appropriate levels of respiratory support for mandatory breaths (Fernández, Miguelena et al. 2013). In intensive care, mechanical ventilation is only one potential intervention and little investigation has been conducted in to the potential use of an Edi signal as a controlling signal for other respiratory interventions, such as HFNC, where patients do not require the delivery of mandatory breaths.

1.3 Purposes

When used in conjunction with other physiological measurements, an Edi signal may be used as part of a more holistic approach for diagnostic WOB assessments and for the development of a patient-driven controlling mechanism for the delivery of HFNC as a main respiratory support mode. It was the objective of a broader clinical study to investigate the impact of HFNC on WOB, in infants with Bronchiolitis, using Edi measurements. The aim of this program of research is to determine the relationship between Edi measurements and other measurements known to correlate with WOB, in assessing WOB under HFNC and non-HFNC conditions. Specifically, using Edi measurements in conjunction with measurements of Respiratory Inductance Plethysmography (RIP) and oesophageal pressure (Poe), the objectives of this work are:

- To quantify the peak (Edi_{MAX}), magnitude (Edi_{AMPL}) and area under the curve (Edi_{AUC}) of the Edi signal under HFNC and non-HFNC conditions, and
- To validate these results with calculations of TAA (using the LLA method), PRP and the diaphragmatic Pressure-Time Product (PTP(di))

1.4 Significance

Closed-loop controlled mechanical ventilation modes, such as NAVA, have the advantage of monitoring and incorporating both ventilator and respiratory parameters to deliver ventilator-triggered breaths that are more closely aligned with the natural breath-to-breath variability of a patient's spontaneous breathing pattern (Suarez-Sipmann 2014). However, current HFNC systems do not have such mechanisms in place to automatically adjust flow rates to meet the patient's inspiratory demand. At present, HFNC flow rates are manually set, as per recommended device guidelines, by clinicians based on a patient's age and weight (Long, Babl et al. 2016) (Riese, Fierce et al. 2015) (Sotello, Orellana-Barrios et al. 2015) (Milési, Boubal et al. 2014). While previous studies have attempted to develop formulas for determining ideal HFNC flow rates (Manley, Dold et al. 2012), to optimise respiratory

support and minimise WOB, further evidence is still needed and dose-finding studies have been suggested to further inform clinical practice. Examining the characteristics of the Edi signal under HFNC and non-HFNC conditions would be the first step to developing an integrated control mechanism for the effective delivery of HFNC therapy. Findings from the broader clinical study, from which this program of research is based, are the first published results describing Edi measurements under HFNC conditions in children under two years of age. This thesis details the specific work conducted to quantify characteristics of Edi signals, under HFNC and non-HFNC conditions, for the purposes of assessing WOB and validates the results against previously established methods for the calculation of WOB.

1.5 Thesis Outline

Chapter 2 contains a literature review of Edi signals, the mechanisms of action of HFNC and the previously established methods for calculating WOB. Chapter 3 outlines the measurement set-up used for the data acquisition of physiological signals and the rationale for each measurement type. Chapter 4 outlines the pertinent results of the broader clinical study which were achieved in relation to the objectives of this program of research. Finally, Chapter 5 contains a discussion of the findings of this program of research as well as insights in to future research directions in this area.

2 LITERATURE REVIEW

This chapter describes the current role of the Edi signal in mechanical ventilation, particularly in relation to the ventilatory mode of NAVA ventilation, and continues with a discussion of its emerging role as a monitoring technology for assessing diaphragmatic work (Section 2.1). This is followed by a discussion of the mechanisms of action of HFNC (Section 2.2) and previously established methods for calculating the WOB under these conditions (Section 2.3).

2.1 NAVA and the Electrical Activity of the Diaphragm

Regarding conventional mechanical ventilation (CMV), it has been shown that even relatively brief periods of controlled CMV can induce ventilator induced diaphragmatic dysfunction (Vassilakopoulos and Petrof 2004). During assisted breathing, equally timed breaths of equal volume are provided, and a patient's WOB is reduced when inspiratory flow from the ventilator exceeds the patient's flow demand. However, patients, particularly those with acute respiratory failure, often have unstable breathing patterns and their requirements for inspiratory flow may change from breath to breath (Kallet, Campbell et al. 2000). Accordingly, new forms of partial mechanical assistance have emerged, where the ventilator contribution is triggered by the patient's respiratory muscles or inspiratory effort, to generate the ventilatory output. Ideally, the respiratory muscles should be active enough to avert the risk of ventilator-induced diaphragmatic dysfunction, and the respiratory rhythm should be under the control of the patient's respiratory centres. Partial mechanical ventilation is aimed to avoid excessive support and guarantee persistent diaphragm activity, enhance patient–ventilation interaction and synchrony, and facilitate the natural breath-to-breath variability, while maintaining adequate gas exchange and optimal patient comfort. The effort exerted by the respiratory muscles directly (as with neurally adjusted ventilatory assist ventilation) or indirectly (as with proportional assist ventilation) drives and regulates ventilator functioning (Terzi and Navalesi 2014).

NAVA is a mode of ventilation whereby the timing and amount of ventilatory assistance is controlled by the patient's neural respiratory drive. In NAVA, the inspiratory assistance is proportional to Edi, which corresponds to muscle fibres depolarization, occurring immediately after the output of the central respiratory centres and just before the intrathoracic pressure variations induced by muscle contraction (Gottfried, Friberg et al. 1999). Using the Edi as the controller signal, NAVA is able to deliver synchronized assistance, both invasively and non- invasively (NIV-NAVA), to follow the variability in breathing pattern, and to monitor patient respiratory drive, independent of leaks. NIV- NAVA, in particular, provides

a truly synchronized mode of non-invasive ventilation, both in time and in level of assistance, and can increase a clinician's ability to treat respiratory failure non-invasively (Sinderby and Beck 2013). Compared with CMV, NAVA results in improved patient-ventilator interaction and synchrony, increased breath-to-breath mechanical variability, enhanced oxygenation and provides lower peak inspiratory pressure, with some evidence suggesting improved patient comfort, less sedation with reduced ventilatory drive, and reduced length of stay (Beck, Emeriaud et al. 2015) (Kallio, Peltoniemi et al. 2015) (Baudin, Pouyau et al. 2015) (Bellani, Coppadoro et al. 2014) (Vagheggini, Mazzoleni et al. 2013) (de la Oliva, Schüffelmann et al. 2012).

Previously, techniques for assessing diaphragmatic work, utilising measurements of trans-diaphragmatic pressure and abdominal volume displacement, have shown inspiratory work to be strongly correlated with the electrical activity of the diaphragm, as measured from its moving average (Guslits, Gaston et al. 1987). The monitoring of Edi is a new minimally invasive bedside technology that was developed for the NAVA mode of ventilation. In addition to its role in NAVA ventilation, this technology provides the clinician with previously unavailable and essential information on diaphragm activity. It allows ventilatory settings to be tailored on an individual basis, avoiding over-assistance, potentially leading to diaphragmatic atrophy. Increased inspiratory Edi levels can also suggest insufficient support, while a strong tonic activity may reflect the patient efforts to increase their lung volume (Larouche, Massicotte et al. 2015). Edi monitoring can play a role in the evaluation of extubation readiness (Wolf, Walsh et al. 2011). Further, Edi monitoring provides the clinician with better understanding of the ventilatory capacity of patients with acute neuromuscular disease (Ducharme-Crevier, Du Pont-Thibodeau et al. 2013). Since infants and young children are predominantly dependent on their diaphragms for respiration, it follows that a signal of the electrical activity of the diaphragm may be used to measure WOB during HFNC treatment and to assess the impact of HFNC on patients and their response to therapy.

2.2 Mechanisms of Action of HFNC

Originally seen as an alternative respiratory support to nasal continuous positive airway pressure (CPAP) for preterm infants, the effectiveness of HFNC has been predominantly studied in this context (Dani, Pratesi et al. 2009) (Saslow, Aghai et al. 2006). Studies comparing HFNC against other oxygen delivery methods such as face mask oxygen, standard nasal cannula, CPAP and other positive pressure devices have been conducted (Bell, Hutchinson et al. 2015) (ten Brink, Duke et al. 2013) (Chang, Cox et al. 2011). However,

unlike traditional NIV devices which use variable flows to generate a fixed CPAP, HFNC systems maintain a fixed flow and generate variable pressures which are not easily monitored (Hasan and Habib 2011). It is proposed that HFNC reduces WOB and improves ventilation efficiency through the following mechanisms of action: (1) washout of the nasopharyngeal dead space, (2) reduction of upper airway resistance, (3) improvement in conductance and pulmonary compliance, (4) reduction in the metabolic work of gas conditioning, and (5) the provision of positive airway pressure (Dysart, Miller et al. 2009).

HFNC systems deliver a heated, humidified oxygen-air mixture at flow rates that may meet or exceed a patient's spontaneous inspiratory flow rate. In infants, flow rates are dependent on the age and weight of the child. Clearing of the nasopharyngeal cavity with flow rates that match or exceed inspiratory demand allows for better consistency in arterial oxygen saturation (SaO_2), improved carbon dioxide (CO_2) clearance and ventilation efficiency. The provision of gas which is pre-heated to body temperature and humidified to 100% relative humidity, reduces the metabolic work associated with gas conditioning, as performed by the nasopharynx under normal respiration. Further, improvements in pulmonary compliance and conductance have been demonstrated (Saslow, Aghai et al. 2006) in contrast with the delivery of gas which is not warmed or humidified (Greenspan, Wolfson et al. 1991). It is believed that the provision of positive distending pressure, or positive end-expiratory pressure (PEEP), can result in improved ventilatory mechanics and assist with gas exchange. Previous studies have demonstrated increases in nasal pharyngeal pressures, oral cavity pressures, end-expiratory oesophageal pressures and tracheal pressures (Groves and Tobin 2007) (Lampland, Plumm et al. 2009) (Kubicka, Limauro et al. 2008) (Parke, McGuinness et al. 2009). However, despite a direct relationship between pharyngeal and airway pressures with increasing flow (Urbano, del Castillo et al. 2012), the degree of positive pressure generated remains inconsistent and can be affected by factors such as the presence of leak around the nares and mouth opening (Hasan and Habib 2011). Regardless of differences in oesophageal pressure, HFNC has a similar effect to CPAP in reducing inspiratory airway resistance through the nasopharynx, which can contribute substantially to WOB. By delivering gas flows that match or exceed a patient's peak inspiratory flow, HFNC minimises this inspiratory resistance by stenting the airways, decreasing the resistive WOB. However, unlike CPAP, HFNC differs during the expiratory phase with increased expiratory pressure serving as a means to increase resistance to expiratory air. For most patients, the generation of positive airway pressure is less likely to be the predominant factor in relieving respiratory distress (Lee, Rehder et al. 2013). The mechanisms of action of HFNC appear to be through

improvements in inspiratory air-flow dynamics and increases in expiratory resistance (Mundel, Feng et al. 2013).

2.3 Determining the Work of Breathing

It is well known that patients who experience less respiratory distress generally recover better overall (Banner, Kirby et al. 1994). Reliable methods for assessing respiratory distress and WOB are essential in formulating appropriate treatments and monitoring response to therapy. Optimised respiratory support aims to reduce WOB by meeting a patient's individual respiratory requirements to maximise their recovery effort while minimising their recovery time. Previously, WOB has been described in terms of the body's oxygen (O_2) cost of breathing of the muscles involved in respiration (Collett, Perry et al. 1985). However, methods for determining metabolic consumption are difficult and unsuitable in an intensive care setting (Cala, Wilcox et al. 1991). Alternative methods, describing the muscle activity involved in respiration, have been developed. In the absence of robust measurement techniques, the determination of respiratory distress includes observational indicators for WOB and is commonly assessed with clinical scoring systems which are generally subjective and based on the clinical experience of the observer (Bueno Campaña, Olivares Ortiz et al. 2014) (Fallot 2005). These indicators may include visual observations of a patient's physical movement of breathing (muscle use, nasal flaring etc.), colour, irritability, feeding and fatigue. Broad states of WOB (usually mild, moderate and severe) are defined, but do not include quantifiable methods of distinguishing WOB levels or established links to commonly monitored physiological parameters (Ravaglia and Poletti 2014).

Thoraco-Abdominal Asynchrony is descriptive of and referred to in clinical scoring systems as chest wall retractions, an observable WOB criterion. It is expressed as a phase angle (θ) of the non-coincident movement of the rib-cage (RC) and abdomen (ABD) during breathing (Hammer and Newth 2009) (Hammer and Eber 2005) and can be used as an indicator of respiratory distress. TAA can be measured non-invasively using Respiratory Inductance Plethysmography, a technique traditionally used in sleep laboratories to describe thoracic and abdominal movements (Reiterer, Sivieri et al. 2015). The technique requires a period of restful breathing for measurement calibration and accuracy is usually only achieved while a subject remains in a single postural position. RIP measurements may be analysed for TAA using the Lissajous Loop Analysis method which is an examination of the loops created by plotting the RC and ABD excursions as an X-Y plot. In normal full-term infants, the RC and ABD expand in synchrony, producing a closed or very narrow loop with a positive slope.

During TAA, the loop opens and may become progressively wider as TAA increases. Paradoxical breathing also creates a closed or very narrow loop, but with a negative slope. Further, the direction of loop rotation indicates which compartment (RC or ABD) precedes the other. Anti-clockwise loops indicate that the ABD compartment (diaphragm) leads the RC, as usually observed in normal quiet breathing and most forms of respiratory distress in children (Hammer and Eber 2005). The LLA method assumes that the RC and ABD signals are sinusoidal. In addition to the LLA method, RIP may be analysed and used to measure tidal volume (V_T) and end-expiratory levels (EEL) and for estimates of respiratory mechanics and WOB (Courtney, Aghai et al. 2003) (Pandit, Courtney et al. 2001) (Saslow, Aghai et al. 2006) (Lavizzari, Veneroni et al. 2014) (Itagaki, Okuda et al. 2014). However, while increasing TAA mirrors the physiological effect on the infant that increasing respiratory loads cause, it does not detect respiratory muscle fatigue.

When respiratory muscles contract, the chest wall expands to produce a pressure difference which allows air to be drawn in to the lungs. Pleural pressures inside the chest wall may be estimated with measurements of oesophageal pressure and calculations derived from these measurements may be used as surrogate measures of WOB (Sassoon, Light et al. 1991). Inspiratory WOB is calculated from the curve of oesophageal pressure versus tidal volume and can be computed using a Campbell diagram. However, this method may underestimate WOB at higher rates of ventilation compared with estimates developed from tracings of the RC and ABD (Goldman, Grimby et al. 1976). Pressure-Time Product (PTP) can be used to measure inspiratory muscle load and is regarded as an index of the oxygen cost of breathing of the respiratory muscles as well as WOB. PTP is calculated as the area subtended by the Poe tracing and the chest wall static recoil pressure for inspiratory time (Sassoon, Light et al. 1991). However, it requires an accurate knowledge of inspiratory flow which cannot be measured with HFNC therapy or in infants and children without an artificial airway. The technique can be modified for non-intubated infants where PTP(mod) is calculated using the maximum negative deflection of Poe and inspiratory time recorded from a RIP device. A further modification allows for the calculation of WOB in both intubated and non-intubated infants to be measured using changes in Poe (pleural pressure) and respiratory rate (RR). The resultant calculation is a Pressure-Time Index (PTI) which is also more accurately referred to as the Pressure-Rate Product. PTI or PRP is an estimate of the energy cost of the WOB because oxygen consumption by muscle is proportional to the integral of muscle tension (or pressure) with respect to time (Klein and Reynolds 1986). Since it is independent of volume related measurements it has the advantage of measuring the work imposed and is a useful

measure in situations where there is a disconnection between respiratory effort and volume (Brochard, Martin et al. 2012). However, as PRP uses an unintegrated pressure signal, it may still underestimate the true WOB. Further, this method of assessing WOB does not account for the added load when intercostal muscle activity is lost and rib cage distortion occurs. It is suggested that the PTI of the diaphragm is a parameter which reflects most of the O_2 consumed by the respiratory muscles during loaded breathing (Collett, Perry et al. 1985) and that PTP(di) is a valid measure of diaphragm unloading, where flow is constant (Fauroux, Hart et al. 2003).

3 METHODS

This chapter describes the measurement methodology which was utilised as part of the broader clinical study, from which this program of research is based. A background to the methodology of the broader clinical study is included in Appendix A.1. Detailed descriptions of the data acquisition components (Figure 1 and Section 3.1) and analysis methods (Section 3.2) adopted to achieve the objectives of this program of research, are presented in this chapter.

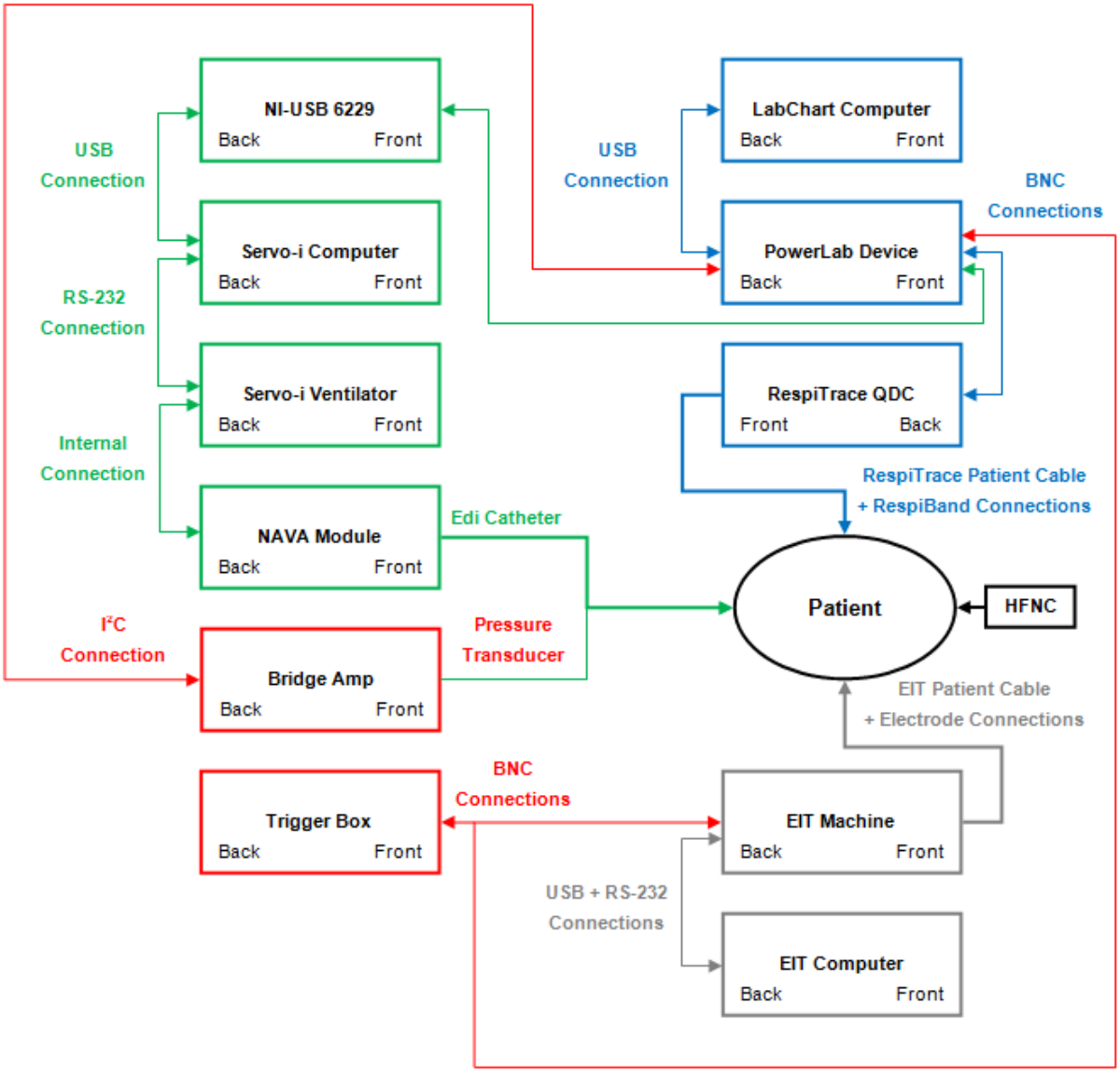

Figure 1: Conceptualised equipment set-up and connection diagram for the broader clinical study from which this program of research is based. Data acquisition techniques used, were for: the electrical activity of the diaphragm, Respiratory Inductance Plethysmography, oesophageal pressure, and Electrial Impedance Tomography.

3.1 Materials and Measurements

3.1.1 HFNC Device

As per standard practice at the primary study site of the broader clinical study, infants were fitted with the appropriate sized nasal cannula (Optiflow Junior Nasal Cannula, Fisher & Paykel Healthcare, Auckland, New Zealand) and the flow rate was commenced through a HFNC circuit (Optiflow Junior RT330, Fisher & Paykel Healthcare, Auckland, New Zealand) at 2L/kg/min (Figure 2). The fraction of inspired oxygen (FiO_2) was titrated to maintain peripheral oxygen saturation (SpO_2) values between 94-98%, and the humidifier was set at 37ºC (MR850, Fisher & Paykel Healthcare, Auckland, New Zealand). For all measurements, mouth closure was obtained either spontaneously or with a pacifier.

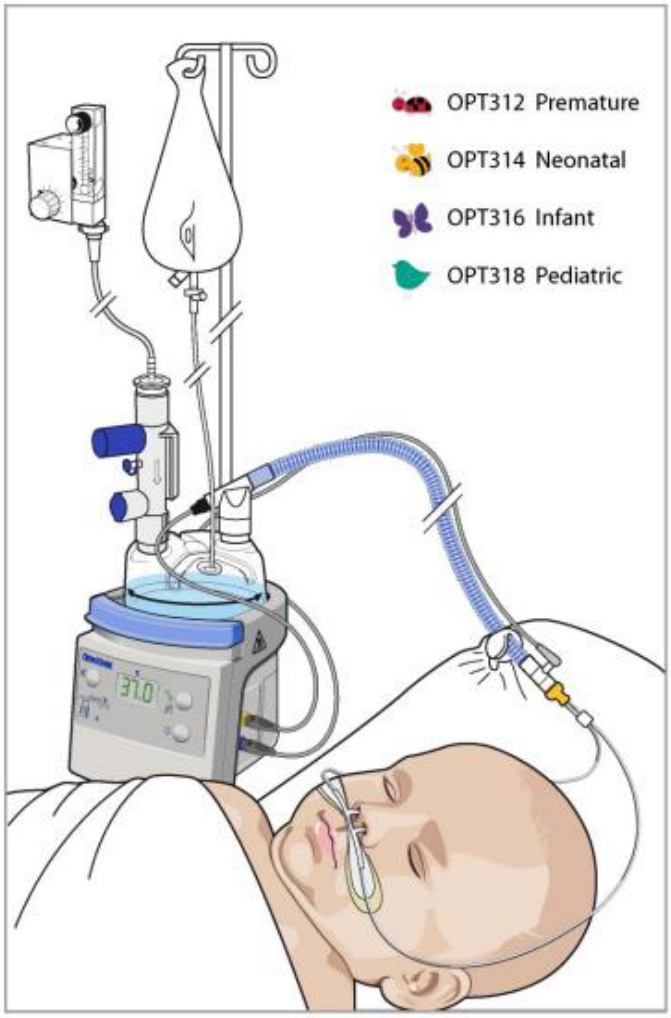

Figure 2: An illustration of the standard High Flow Nasal Cannula system, used in the broader clinical study from which this program of research is based, manufactured by Fisher & Paykel Healthcare. (https://www.fphcare.com.au)

3.1.2 Electrical Activity of the Diaphragm

The Edi signal was measured using an appropriate sized Edi catheter, a nasogastric probe designed for use with the NAVA module of a Servo-i ventilator (Maquet Critical Care, Solna, Sweden). The Edi catheter was inserted through the nose, to the level of the diaphragm, and the non-inserted portion was taped to the side of the patient's face to ensure stability of probe placement. When positioned correctly, the neural excitation of the diaphragm is captured by an array of electrodes fitted at the end of the Edi catheter, is filtered and processed by the NAVA module and then relayed to the Servo-i ventilator (Figure 3). For the Edi signal to be recorded simultaneously with other data signals for analysis, the resultant Edi signal from the Servo-i Ventilator was then fed to a laptop computer running ventilator performance data software (Servo Tracker v4.1, Maquet Critical Care, Solna, Sweden) and then on to a PowerLab 16/35 Series analogue recording device (ADInstruments Ltd, Dunedin, New Zealand) via the use of a USB 6229 BNC communications module (National Instruments Corporation, Texas, USA). The Edi signal was examined for determinants of respiratory drive where increased diaphragm activity is indicated by increased values of Edi_{MAX} and Edi_{AMPL}.

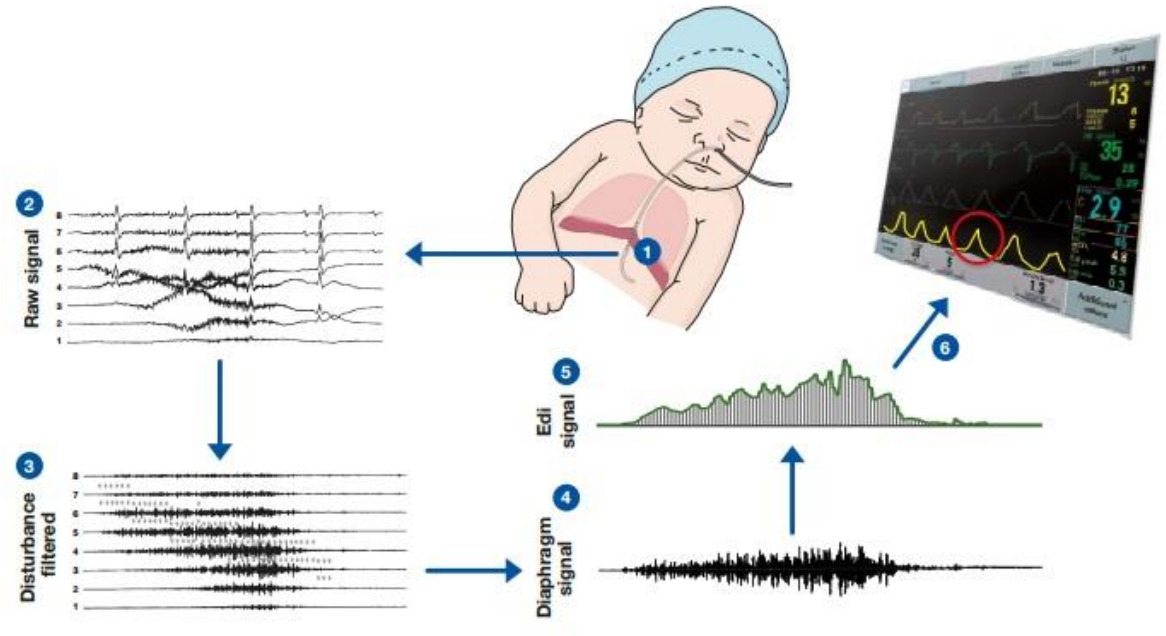

Figure 3: An illustration of the Edi monitoring function of a Servo-i ventilator, manufactured by MAQUET, which was used in isolation to monitor the Edi signal of patients receiving High Flow Nasal Cannula therapy. (http://www.maquet.com)

3.1.3 Respiratory Inductance Plethysmography

A respiratory inductance plethysmograph, Respitrace Q.D.C. (CareFusion Corporation, San Diego, USA), with self-calibration functionality was used to determine respiratory movement and asynchrony. Two separate bands, XactTrace Disposable Belts (Embla, Denver, USA), were placed; one around the chest circumference between the armpits and nipple level and one around the abdomen at navel level (Figure 4). For consistency, measurements were taken with infants lying in the supine position. Physiological data generated by the RIP are waveforms representative of the RC, ABD and overall respiratory (SUM) movement. The RIP_{SUM} signal was used as the main respiratory waveform in subsequent analyses and the RIP_{RC} and RIP_{ABD} signals were used in the calculation of θ for TAA, using the LLA method. These RIP signals were fed directly from the Respitrace Q.D.C. to the PowerLab device via BNC cables.

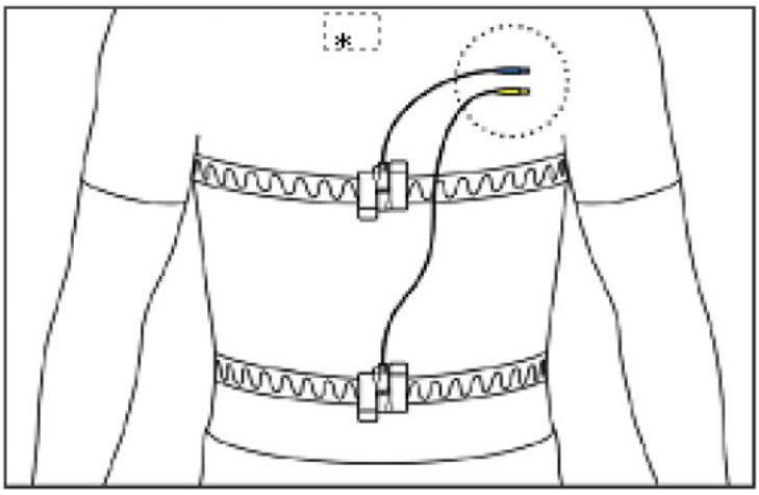

Figure 4: An illustration of the placement of disposable bands used in the measurement of Respiratory Inductance Plethysmography (http://www.mortara.com/au).

3.1.4 Oesophagus Pressures

Poe measurements were taken as an indirect measure of CPAP. The Edi catheter, which has a side port used for nasogastric tube (NG) feeds, was connected to a pressure transducer and pulled back to the distal third of the oesophagus to achieve a waveform that was free from cardiac artefact. Feeds were discontinued for the length of the study. To maintain patency of the Edi catheter, a normal saline flush at a rate of 1mL/hr was applied. The Poe signal was fed into the PowerLab device and then calibrated and zeroed to atmospheric pressure. The Poe signal was used in conjunction with the RIP_{SUM} signal for calculations of PRP and PTP(di) as well as the intrinsic Positive End-Expiratory Pressure (PEEPi).

3.1.5 Electrical Impedance Tomography

As with other clinical studies, previously conducted by the investigators of the broader clinical study, a Goe-MF II Electrical Impedance Tomography (EIT) system (Cardinal Health, Hoechberg, Germany) was used as a non-invasive monitoring tool to examine the regional ventilation distribution and regional filling characteristics of the lungs (Schibler, Yuill et al. 2009, Grant, Pham et al. 2011, Humphreys, Pham et al. 2011, Pham, Yuill et al. 2011, Hough, Johnston et al. 2012, Schibler, Pham et al. 2013, Hough, Pham et al. 2014). Sixteen electrocardiography (ECG) electrodes were placed equidistantly around the chest circumference, at nipple level, and a 75 kHz injection frequency of $5mA_{pk-pk}$ was used to produce functional images of relative impedance changes at a rate of 13 images per second (13 Hz) (Figure 5). Due to the complexity and limitations of the EIT system, measurements were recorded on to a separate EIT-dedicated laptop computer. However, to synchronise the EIT recordings with the rest of the study measurements, a 1.5 V marker signal was applied to both the sole analogue channel of the EIT system as well as to one of the available channels on the PowerLab device via BNC cables. All EIT measurements were recorded with infants lying in the supine position.

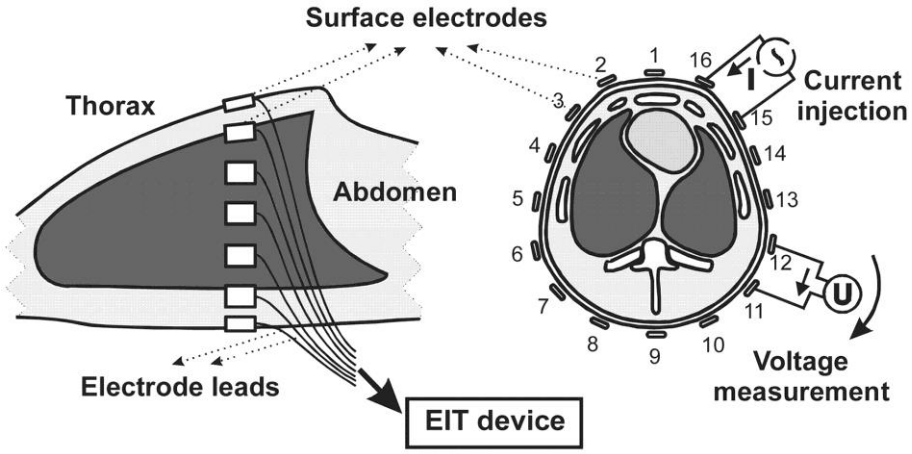

Figure 5: An illustration of the ECG electrode placement used in the measurement of Electrical Impedance Tomography (Frerichs, Hinz et al. 2002).

3.1.6 Data Acquisition using PowerLab

All waveforms channelled in to the PowerLab device were recorded using the accompanying data acquisition and analysis software, LabChart v6.1 (ADInstruments Ltd, Dunedin, New Zealand). All PowerLab signals were sampled at 1 kHz.

3.2 Measurement Analysis

As per the design of the broader clinical study (Appendix A.1), a treatment (Bronchiolitis) group and control (Cardiac) group of infants, with and without clinical signs of increased WOB respectively, were measured off and on HFNC therapy. For each change in HFNC state, a period of 5 minutes was allowed for stabilisation and data was recorded for 10 minutes to capture periods of undisturbed regular breathing for analysis. In accordance with analysis conventions set by the investigators of the broader clinical study, waveform segments of at least ten contiguous breaths, with little variation in segment baseline and breath-to-breath amplitude (Frerichs, Schiffmann et al. 2003), were identified at the end of each set of measurements and used for analysis as follows.

3.2.1 Edi, RIP_{SUM} and Poe

Basic parameters such as the breath-to-breath minimum, maximum, amplitude, rate, and area under the curve (AUC) were calculated. These parameters, as calculated for the Edi signal, were: the end-expiratory level Edi (Edi_{MIN}), the inspiratory maximum Edi (Edi_{MAX}), Edi amplitude (Edi_{AMPL}), breath-to-breath respiratory rate Edi (Edi_{RR}) and breath-to-breath Edi AUC (Edi_{AUC}).

Similar parameters, calculated for the overall respiratory movement (RIP_{SUM}) signal, were: the end-expiratory level (RIP_{MIN}, also referred to as RIP_{EEL}), the inspiratory peak (RIP_{MAX}), amplitude of tidal breathing (RIP_{AMPL}), breath-to-breath respiratory rate (RIP_{RR}) and breath-to-breath AUC (RIP_{AUC}). Additional RIP_{SUM} parameters calculated were: the inspiratory time to peak (RIP_{Ti}), the respiratory cycle length (RIP_{Ttot}), and the ratio between the inspiratory-phase to length of entire respiratory cycle ($RIP_{Ti/Ttot}$).

Parameters calculated for the Poe signal were: the minimum respiratory Poe point (Poe_{MIN}), the maximum respiratory Poe point (Poe_{MAX}), and the breath-to-breath change in Poe amplitude (Poe_{AMPL}).

3.2.2 Traditional WOB Calculations

Traditional measures for assessing WOB were derived from the Poe and RIP signals (Figure 6) (Pham, O'Malley et al. 2015). The Pressure-Rate Product, which is often used as a simplified method of examining WOB, was calculated as Poe_{AMPL} multiplied by RR (Klein and Reynolds 1986). The Pressure-Time Product of the diaphragm was used to examine the inspiratory WOB and was calculated as the integral of the Poe curve during inspiration ($\int Poe_{INSP}$) multiplied by RR (Collett, Perry et al. 1985). The intrinsic Positive End-Expiratory

Pressure was calculated as the difference between Poe_{MAX} and the Poe at the start of inspiration, as defined by the RIP_{SUM} signal i.e. the drop in Poe during the short time period when no inspiratory volume change on the RIP_{SUM} signal could be observed (Collett, Perry et al. 1985).

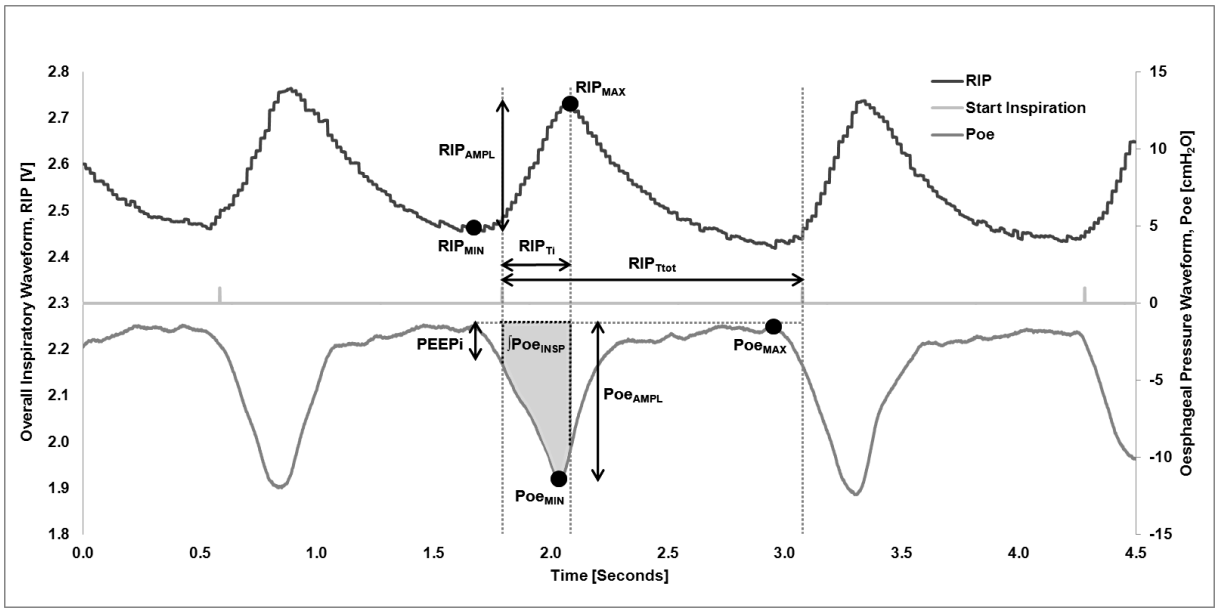

Figure 6: Representative overall inspiratory RIP_{SUM} and oesophageal pressure (Poe) waveforms with a signal showing the start of inspiration. For each breath, the respiratory rate (RR) was determined from the total length of respiration as defined by the overall inspiratory waveform (RIP_{Ttot}). The Pressure-Rate Product is calculated as the oesophageal pressure amplitude multiplied by the respiratory rate, PRP = Poe_{AMPL} x RR. The intrinsic Positive End-Expiratory Pressure (PEEPi) is defined as the difference between the maximum oesophageal pressure and the oesophageal pressure at the start of inspiration. The diaphragmatic Pressure-Time Product is calculated as the area subtended by the oesophageal pressure waveform during inspiration (taking into account the PEEPi) multiplied by the respiratory rate, PTP(di) = $\int Poe_{INSP}$ x RR. The ratio of inspiratory time to total inspiratory time was determined from the overall inspiratory waveform, $RIP_{Ti/Ttot} = RIP_{Ti} / RIP_{Ttot}$. (Pham, O'Malley et al. 2015)

3.2.3 Lissajous Loop Analysis

Thoraco-Abdominal Asynchrony is descriptive of chest wall retractions which are an observable WOB criteria included in clinical assessments for respiratory distress. It is assessed using the Lissajous Loop Analysis method and is expressed as a phase angle, θ, of the non-coincident movement of the ribcage and abdomen (Prisk, Hammer et al. 2002). Specifically, from an X-Y plot of the RC and ABD excursions, θ is calculated as the arcsine of the distance traversed by the ABD at the mid-point of the overall RC excursion (m), divided by the overall ABD excursion (s) (Figure 7) (Hammer and Eber 2005). However,

despite the range of commercial tools and modules available for data analysis, no specific tools exist for the performance of LLA analysis in LabChart. Consequently, for this program of research, a specific series of LabChart macros were developed and implemented to perform the required phase angle analysis, using the LLA method. For completeness, further data analysis macros were also developed using Visual Basic for Applications (VBA) in Microsoft Excel, to collate data and perform additional calculations. Additional parameters, calculated during the step-wise implementation of the LLA method, were: the minimum RC point (RC_{MIN}), the maximum RC point (RC_{MAX}), the RC excursion length (RC_{AMPL}), the minimum ABD point (ABD_{MIN}), the maximum ABD point (ABD_{MAX}), the ABD excursion length (ABD_{AMPL}), the Area Inside the Loop and the Slope of the Loop.

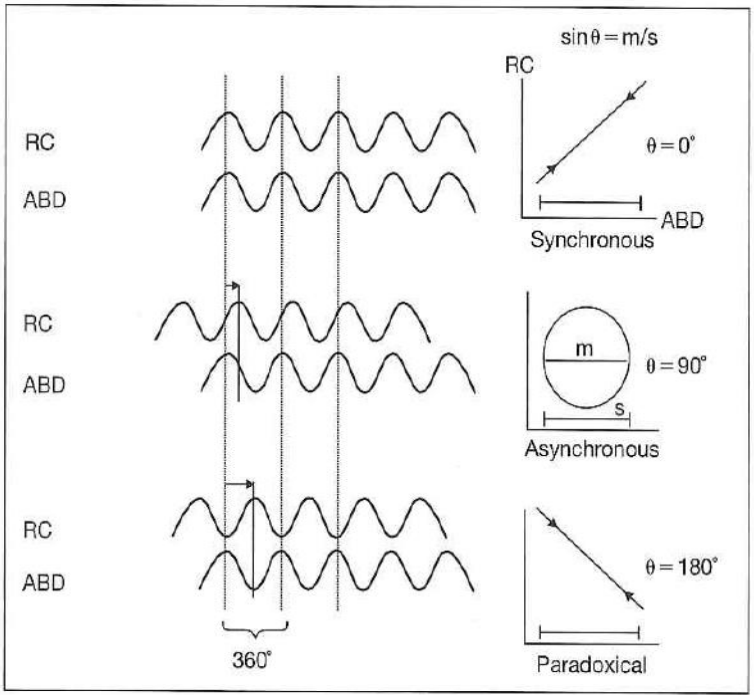

Figure 7: The phase angle of TAA is calculated from the equation sin θ = m/s, where m is the distance traversed by the ABD at the mid-point of the RC excursion and s is the overall ABD excursion (Hammer and Eber 2005).

3.2.4 EIT

EIT measurements were analysed separately using an EIT Data Analyser program, previously developed by me, for the broader clinical study investigators, in MATLAB. However, a subset of the pre-processed EIT waveforms was also up-sampled, synchronised, and input to LabChart for integrated analysis. Namely, waveforms representative of the overall respiratory movement (EIT_{GLOBAL}), the anterior region of the lungs ($EIT_{ANTERIOR}$) and the posterior regions of the lungs ($EIT_{POSTERIOR}$) were analysed in LabChart, examining the breath-to-

breath minimums, maximums and amplitudes of each signal. For completeness, it is noted that EIT analysis methods, as standardised by the broader clinical study investigators, were written by me and includes examinations of regional end-expiratory level, regional tidal volume amplitudes, asynchrony between lung compartments (expressed as a Phase Angle, α), distribution profiles of relative impedance change, and calculations for the geometric centre of ventilation (GC), regional filling indices (FI) and the global inhomogeneity index (GI) (Schibler, Yuill et al. 2009, Grant, Pham et al. 2011, Humphreys, Pham et al. 2011, Pham, Yuill et al. 2011, Hough, Johnston et al. 2012, Schibler, Pham et al. 2013, Hough, Pham et al. 2014).

3.3 Implementation in LabChart

For this program of research, the Edi, RIP, Poe and subset EIT signals were analysed using a specific sequence of LabChart and Excel based macros, developed by me. A detailed description of the particular series of LabChart macros, incorporating the LLA method for calculating phase angles, is included in Appendix A.2.

3.4 Statistics

Unless otherwise stated, data is presented as a mean and 95% confidence interval (CI). Paired samples t-Test was applied for parameters measured off and on HFNC therapy, for infants with Bronchiolitis (the treatment group) and Cardiac infants (the control group), and a univariate ANOVA was used to compare data between subgroups within each HFNC state (SPSS 15.0 for Windows). A p-value of <0.05 was considered to be statistically significant.

4 RESULTS

4.1 Electrical Activity of the Diaphragm

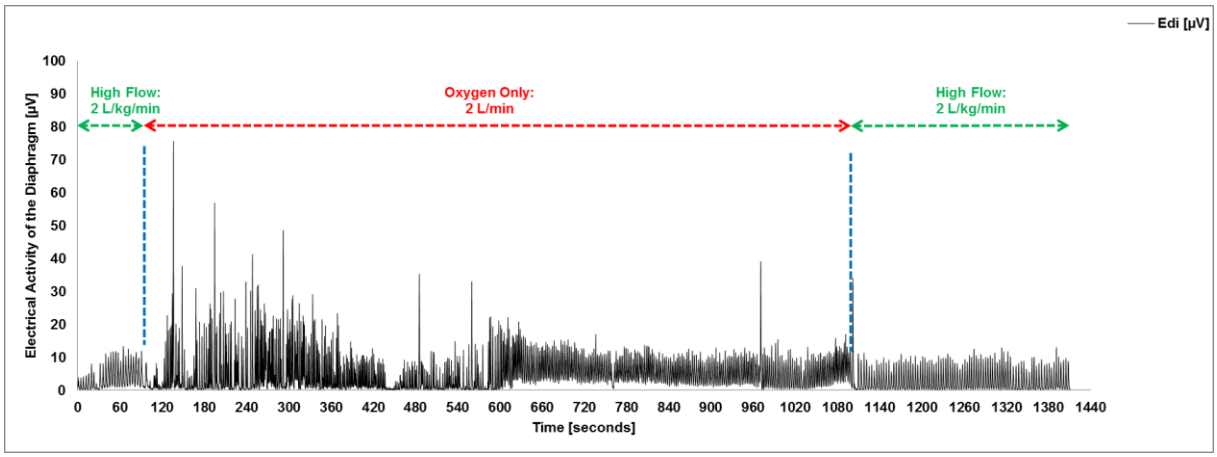

Figure 8: Representative recording of the electrical activity of the diaphragm showing the effect of removing and reapplying HFNC therapy.

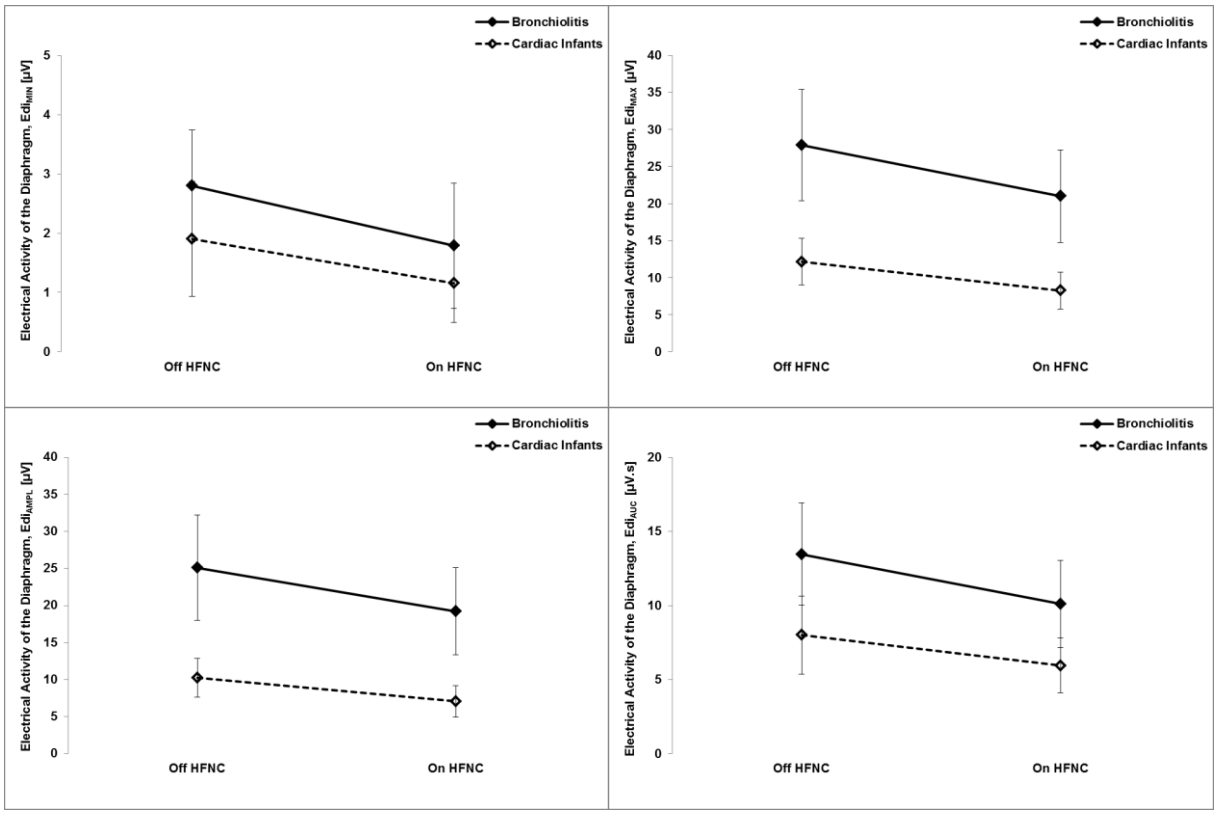

Figure 9: Mean values of the electrical activity of the diaphragm for infants with Bronchiolitis and Cardiac infants, off and on HFNC. Mean and 95% confidence intervals are shown.

Overall, the measured changes off and on HFNC in Edi_{MAX}, Edi_{AMPL} and Edi_{AUC} were significantly higher in infants with Bronchiolitis compared to Cardiac infants, whereas the

measured changes in Edi_{MIN} and Edi_{RR} were not (Figure 9). Within the group of infants with Bronchiolitis, significant decreases from off HFNC to on HFNC were observed in the Edi_{MIN}, Edi_{MAX}, Edi_{AMPL}, Edi_{RR} and Edi_{AUC}. Within the group of Cardiac infants, similar but less prominent changes in electrical diaphragmatic activity were observed (Table 1).

Table 1: Mean values and absolute mean changes of the electrical activity of the diaphragm for infants with Bronchiolitis and Cardiac infants, off and on HFNC. Paired samples t-Tests were used to compare HFNC states within groups (*). An ANOVA was used to compare mean changes between groups (^). A p-value of <0.05 was considered to be statistically significant.

	Bronchiolitis		Cardiac Infants		Between Groups	
	Off HFNC *Mean*	On HFNC *Mean*	Off HFNC *Mean*	On HFNC *Mean*	Bronchiolitis *|Δ Mean|*	Cardiac *|Δ Mean|*
Edi_{MIN} [µV]	2.798	1.789	1.902	1.156	1.009	0.746
p-value	0.010*		0.004*		0.118	
Edi_{MAX} [µV]	27.879	20.995	12.155	8.244	6.884	3.911
p-value	0.017*		<0.001*		<0.001^	
Edi_{AMPL} [µV]	25.081	19.206	10.253	7.088	5.875	3.165
p-value	0.021*		<0.001*		<0.001^	
Edi_{RR} [BPM]	61.236	55.275	52.325	44.483	5.961	7.842
p-value	0.003*		0.067		0.061	
Edi_{AUC} [µV.s]	13.453	10.114	8.012	5.956	3.339	2.056
p-value	0.006*		0.001*		0.002^	

4.2 Respiratory Inductance Plethysmography

In comparing infants with Bronchiolitis to Cardiac infants, the measured changes off and on HFNC in RIP_{MIN}, RIP_{MAX}, RIP_{AMPL} and $RIP_{Ti/Ttot}$ were not significantly different (Figure 10). However, infants with Bronchiolitis showed a significant increase in end-expiratory level RIP_{MIN}, between HFNC states whereas the group of Cardiac infants only showed a moderate but not significant increase. In infants with Bronchiolitis: a significant increase in RIP_{MIN} and RIP_{AUC} and a significant decrease in RIP_{MAX}, RIP_{AMPL}, RIP_{RR}, and $RIP_{Ti/Ttot}$ were observed from off HFNC to on HFNC. In the group of Cardiac infants, only the RIP_{AMPL} and $RIP_{Ti/Ttot}$ showed a significant decrease (Table 2).

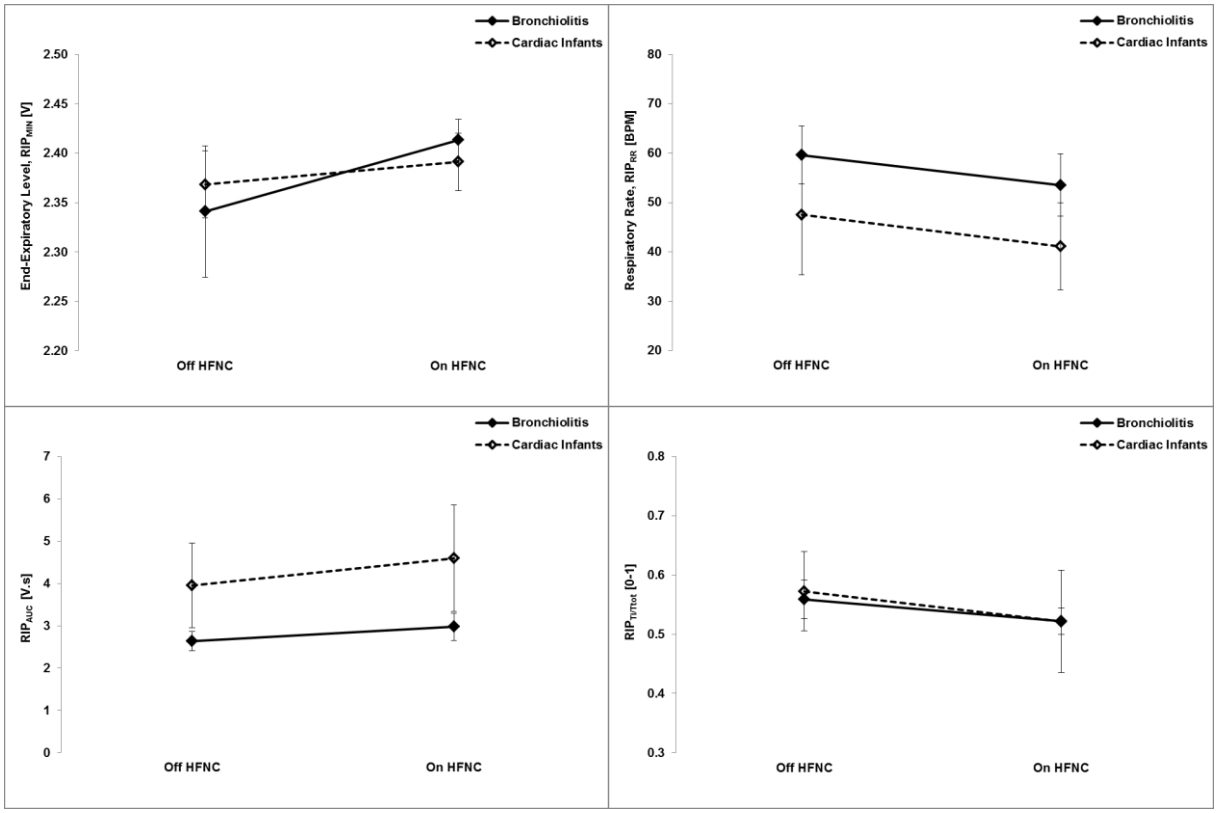

Figure 10: Mean values of the overall Respiratory Inductance Plethysmography waveform (RIP_{SUM}) for infants with Bronchiolitis and Cardiac infants, off and on HFNC. Mean and 95% confidence intervals are shown.

Table 2: Mean values and absolute mean changes in the Respiratory Inductance Plethysmography measurements taken for infants with Bronchiolitis and Cardiac infants, off and on HFNC. Paired samples t-Tests were used to compare HFNC states within groups (*). An ANOVA was used to compare mean changes between groups (^). A p-value of <0.05 was considered to be statistically significant.

	Bronchiolitis		Cardiac Infants		Between Groups	
	Off HFNC *Mean*	On HFNC *Mean*	Off HFNC *Mean*	On HFNC *Mean*	Bronchiolitis *|Δ Mean|*	Cardiac *|Δ Mean|*
RIP_{MIN} [V]	2.341	2.413	2.368	2.391	0.072	0.023
p-value	0.012*		0.113		0.905	
RIP_{MAX} [V]	2.793	2.745	2.768	2.742	0.048	0.026
p-value	0.046*		0.149		0.689	
RIP_{AMPL} [V]	0.452	0.332	0.399	0.350	0.120	0.049
p-value	0.017*		0.025*		0.729	
RIP_{RR} [BPM]	59.584	53.513	47.547	41.101	6.071	6.446
p-value	0.004*		0.084		0.008^	
RIP_{AUC} [V.s]	2.635	2.977	3.951	4.591	0.342	0.640
p-value	0.003*		0.059		0.001^	
RIP_{Ti} [ms]	528.988	564.095	806.719	824.912	35.107	18.193
p-value	0.125		0.428		0.015^	
RIP_{Ttot} [ms]	947.507	1076.245	1387.971	1579.446	128.738	191.475
p-value	0.006*		0.073		0.005^	
$RIP_{Ti/Ttot}$ [0-1]	0.559	0.522	0.572	0.521	0.037	0.051
p-value	0.025*		0.017*		0.829	

4.3 Oesophagus Pressure

Between infants with Bronchiolitis and Cardiac infants, the measured changes off and on HFNC in Poe_{MIN}, Poe_{MAX}, Poe_{AMPL} and PEEPi were not significantly different, whereas changes in the traditional measures of WOB, PRP and PTP(di), were (Figure 11). In infants with Bronchiolitis, Poe_{MIN} increased from off HFNC to on HFNC, Poe_{MAX} remained relatively similar, and Poe_{AMPL} decreased. Similarly, in Cardiac infants, Poe_{MIN} increased, Poe_{MAX} remained unchanged and Poe_{AMPL} decreased. For traditional measures of WOB, the PRP and PTP(di) decreased significantly in infants with Bronchiolitis. In Cardiac infants, similar but less prominent changes were observed. With both groups, PEEPi decreased from off HFNC to on HFNC (Table 3).

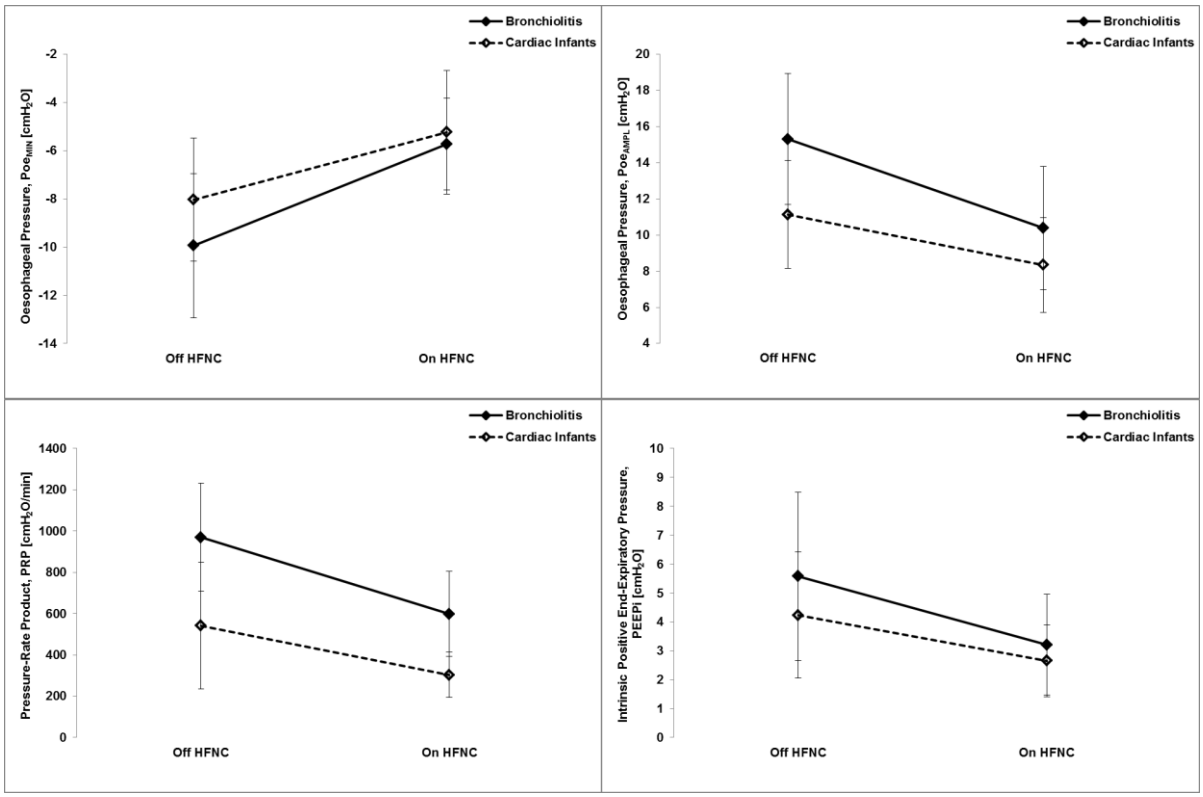

Figure 11: Mean values in the Oesophageal Pressure waveform and related WOB calculations for infants with Bronchiolitis and Cardiac infants, off and on HFNC. Mean and 95% confidence intervals are shown.

Table 3: Mean values and absolute mean changes of the oesophageal pressure calculations for infants with Bronchiolitis and Cardiac infants, off and on HFNC. Paired samples t-Tests were used to compare HFNC states within groups (*). An ANOVA was used to compare mean changes between groups (^). A p-value of <0.05 was considered to be statistically significant.

	Bronchiolitis		Cardiac Infants		Between Groups	
	Off HFNC *Mean*	On HFNC *Mean*	Off HFNC *Mean*	On HFNC *Mean*	Bronchiolitis *|Δ Mean|*	Cardiac *|Δ Mean|*
Poe_{MIN} [cmH_2O]	-9.936	-5.727	-8.036	-5.236	4.209	2.800
p-value	0.001*		0.040*		0.393	
Poe_{MAX} [cmH_2O]	5.379	4.667	3.095	3.104	0.712	0.009
p-value	0.266		0.495		0.172	
Poe_{AMPL} [cmH_2O]	15.315	10.393	11.131	8.340	4.922	2.791
p-value	0.001*		0.039*		0.078	
PRP [cmH_2O/min]	969.647	598.450	540.726	302.679	371.197	238.047
p-value	0.004*		0.074		0.007^	
PTP [cmH_2O.s/min]	228.302	148.896	124.825	82.311	79.406	42.514
p-value	0.003*		0.046*		0.006^	
PEEPi [cmH_2O]	5.573	3.206	4.230	2.651	2.367	1.579
p-value	0.032*		0.112		0.399	

4.4 Lissajous Loop Analysis

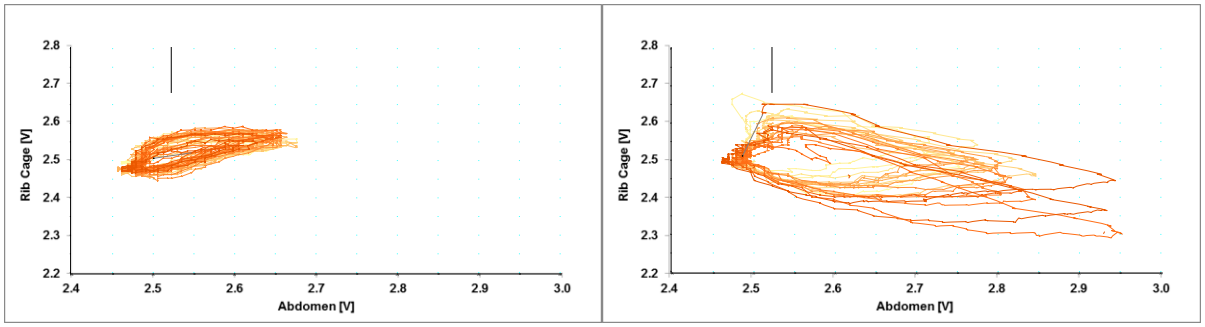

(a) A Bronchiolitis infant, off and on HFNC.

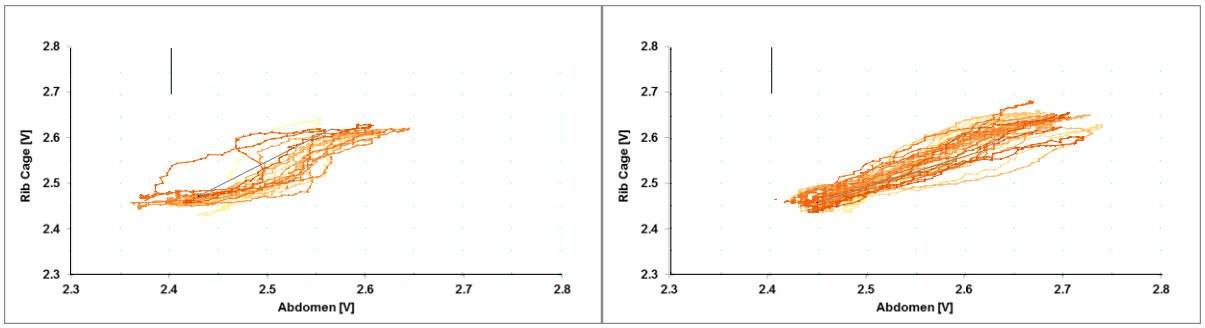

(b) A Cardiac Infant, off and on HFNC

Figure 12: Representative Lissajous Loops of the rib cage and abdomen signals on an X-Y plot, taken from Respiratory Inductance Plethysmography recordings, for an infant with Bronchiolitis and a Cardiac infant, off and on HFNC.

In calculating the phase angle of TAA using the LLA method, a number of step-wise calculations were conducted and additional waveform parameters examined. However, between infants with Bronchiolitis and Cardiac infants, no significant differences in the measured changes off and on HFNC were found (Table 4). In infants with Bronchiolitis, RC_{MAX} and RC_{AMPL} decreased from off HFNC to on HFNC. The calculated phase angle also decreased from off HFNC to on HFNC but the finding was not statistically significant. In Cardiac infants, RC_{MIN} increased while RC_{AMPL} and the distance traversed by the ABD signal at the mid-point of the RC excursion decreased. It is of note that θ also decreased from off HFNC to on HFNC (Figure 13).

Table 4: Mean values and absolute mean changes of the Lissajous Loop Analysis related calculations for infants with Bronchiolitis and Cardiac infants, off and on HFNC. Paired samples t-Tests were used to compare HFNC states within groups (*). An ANOVA was used to compare mean changes between groups (^). A p-value of <0.05 was considered to be statistically significant.

	Bronchiolitis		Cardiac Infants		Between Groups	
	Off HFNC *Mean*	On HFNC *Mean*	Off HFNC *Mean*	On HFNC *Mean*	Bronchiolitis *|Δ Mean|*	Cardiac *|Δ Mean|*
RC_{MIN} [V]	2.368	2.410	2.373	2.411	0.042	0.038
p-value	0.066		0.021*		0.884	
RC_{MAX} [V]	2.694	2.653	2.651	2.633	0.041	0.018
p-value	0.029*		0.136		0.320	
RC_{AMPL} [V]	0.326	0.242	0.278	0.222	0.084	0.056
p-value	0.044*		0.009*		0.459	
ABD_{MIN} [V]	2.430	2.445	2.435	2.441	0.015	0.006
p-value	0.100		0.252		0.931	
ABD_{MAX} [V]	2.636	2.649	2.683	2.631	0.013	0.052
p-value	0.332		0.126		0.622	
ABD_{AMPL} [V]	0.207	0.204	0.248	0.191	0.003	0.057
p-value	0.468		0.088		0.666	
m [V]	0.143	0.119	0.169	0.087	0.024	0.082
p-value	0.160		0.018*		0.910	
s [V]	0.207	0.204	0.248	0.191	0.003	0.057
p-value	0.468		0.088		0.666	
Area Inside Loop	0.025	0.021	0.030	0.020	0.004	0.010
p-value	0.227		0.117		0.763	
Slope	1.360	0.454	0.844	1.205	0.906	0.361
p-value	0.155		0.201		0.789	
θ [°]	56.038	44.229	63.493	27.395	11.809	36.098
p-value	0.200		0.007*		0.689	

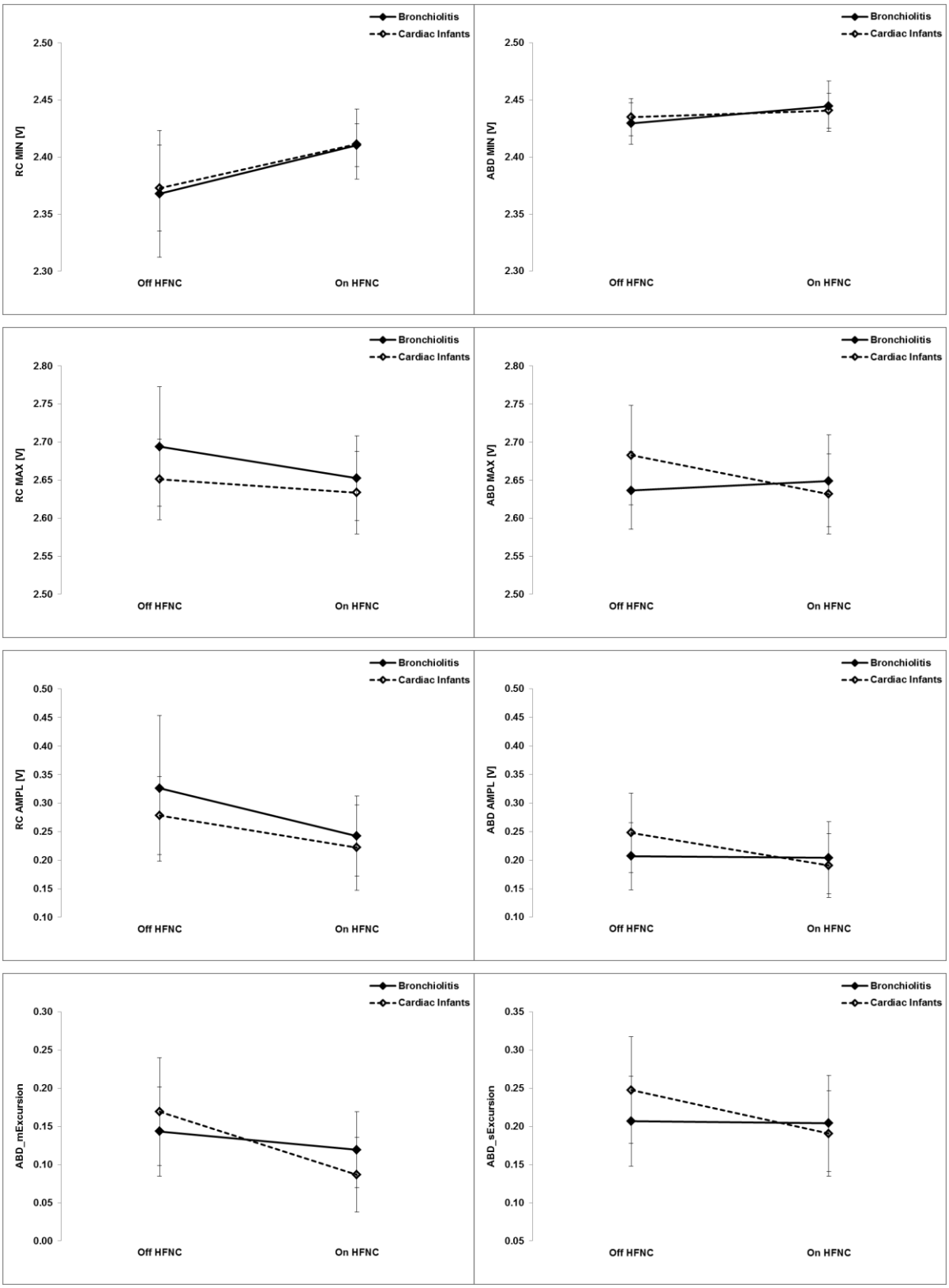
Bronchiolitis
Cardiac Infants
RC MIN [V]
2.50
2.45
2.40
2.35
2.30
Off HFNC
On HFNC
Bronchiolitis
Cardiac Infants
ABD MIN [V]
2.50
2.45
2.40
2.35
2.30
Off HFNC
On HFNC
Bronchiolitis
Cardiac Infants
RC MAX [V]
2.80
2.75
2.70
2.65
2.60
2.55
2.50
Off HFNC
On HFNC
Bronchiolitis
Cardiac Infants
ABD MAX [V]
2.80
2.75
2.70
2.65
2.60
2.55
2.50
Off HFNC
On HFNC
Bronchiolitis
Cardiac Infants
RC AMPL [V]
0.50
0.45
0.40
0.35
0.30
0.25
0.20
0.15
0.10
Off HFNC
On HFNC
Bronchiolitis
Cardiac Infants
ABD AMPL [V]
0.50
0.45
0.40
0.35
0.30
0.25
0.20
0.15
0.10
Off HFNC
On HFNC
Bronchiolitis
Cardiac Infants
ABD_mExcursion
0.30
0.25
0.20
0.15
0.10
0.05
0.00
Off HFNC
On HFNC
Bronchiolitis
Cardiac Infants
ABD_sExcursion
0.35
0.30
0.25
0.20
0.15
0.10
0.05
Off HFNC
On HFNC

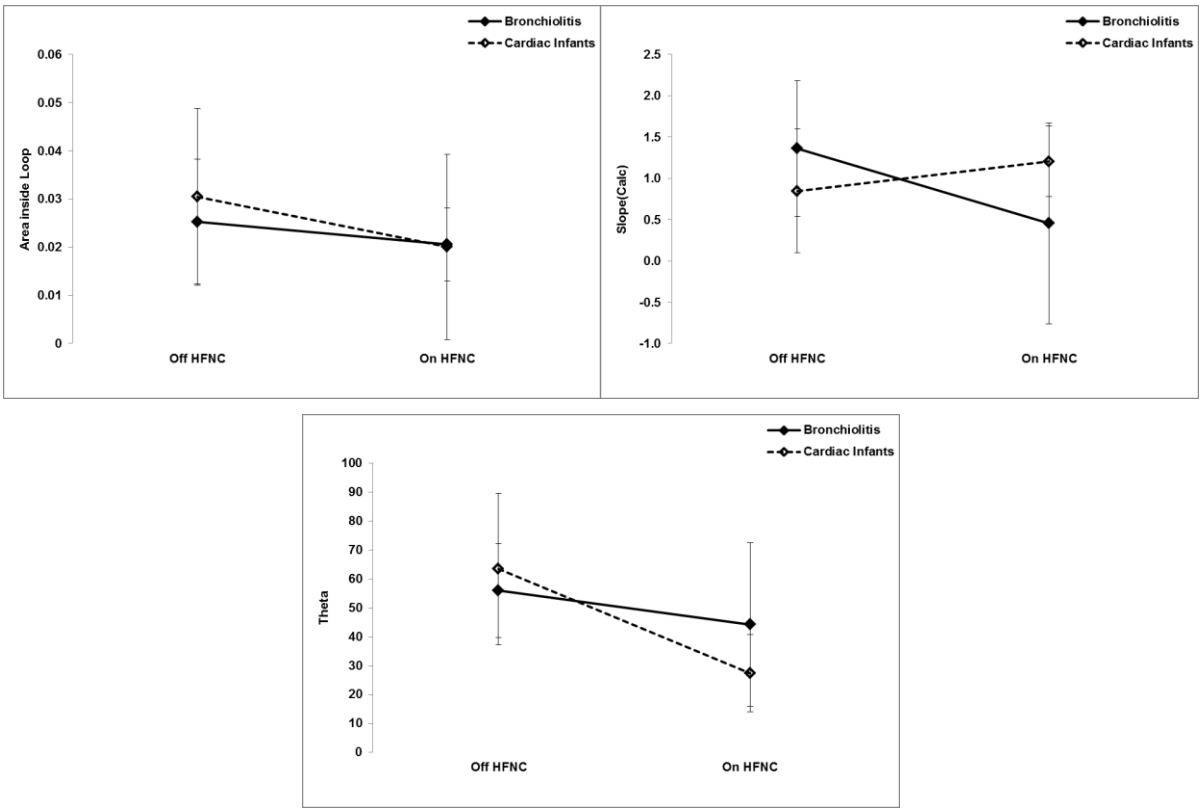

Figure 13: Mean values of the Lissajous Loop Analysis related calculations for infants with Bronchiolitis and Cardiac infants, off and on HFNC. Mean and 95% confidence intervals are shown.

4.5 Electrical Impedance Tomography

EIT analysis, as standardised by the investigators of the broader clinical study, was conducted separately. Since EIT is a monitoring technology used primarily to describe ventilation distribution and lung mechanics, and not for describing indicators associated with WOB, the main results of this analysis are presented in Appendix A.3. However, for completeness, results from the subset of pre-processed EIT signals, which were included with the main LabChart analysis, are presented below (Table 5).

Table 5: Mean values and absolute mean changes in the pre-processed Electrical Impedance Tomography waveforms[1] for infants with Bronchiolitis and Cardiac infants, off and on HFNC. Paired samples t-Tests were used to compare HFNC states within groups (*). An ANOVA was used to compare mean changes between groups (^). A p-value of <0.05 was considered to be statistically significant.

	Bronchiolitis		Cardiac Infants		Between Groups	
	Off HFNC *Mean*	On HFNC *Mean*	Off HFNC *Mean*	On HFNC *Mean*	Bronchiolitis *|Δ Mean|*	Cardiac *|Δ Mean|*
G_{MIN} [ΔZ]	-0.017	0.003	0.002	0.013	0.020	0.011
p-value	0.065		0.103		0.198	
G_{MAX} [ΔZ]	0.016	0.030	0.047	0.055	0.014	0.008
p-value	0.157		0.213		0.014^	
G_{AMPL} [ΔZ]	0.033	0.027	0.045	0.042	0.006	0.003
p-value	0.034*		0.265		0.036^	
A_{MIN} [ΔZ]	-0.019	0.008	-0.023	0.006	0.027	0.029
p-value	0.063		0.002*		0.806	
A_{MAX} [ΔZ]	0.012	0.033	0.019	0.045	0.021	0.026
p-value	0.142		0.003*		0.419	
A_{AMPL} [ΔZ]	0.030	0.024	0.042	0.039	0.006	0.003
p-value	0.043*		0.246		0.069	
P_{MIN} [ΔZ]	-0.023	-0.005	0.021	0.022	0.018	0.001
p-value	0.141		0.464		0.019^	
P_{MAX} [ΔZ]	0.019	0.028	0.070	0.067	0.009	0.003
p-value	0.295		0.403		0.008^	
P_{AMPL} [ΔZ]	0.042	0.034	0.049	0.045	0.008	0.004
p-value	0.013*		0.199		0.202	

[1] Pre-processed Electrical Impedance Tomography waveforms, representative of the Global (G), Anterior (A) and Posterior (P) regions of the lungs, were examined for minima (G_{MIN}, A_{MIN}, P_{MIN}), maxima (G_{MAX}, A_{MAX}, P_{MAX}) and amplitude values (G_{AMPL}, A_{AMPL}, P_{AMPL}).

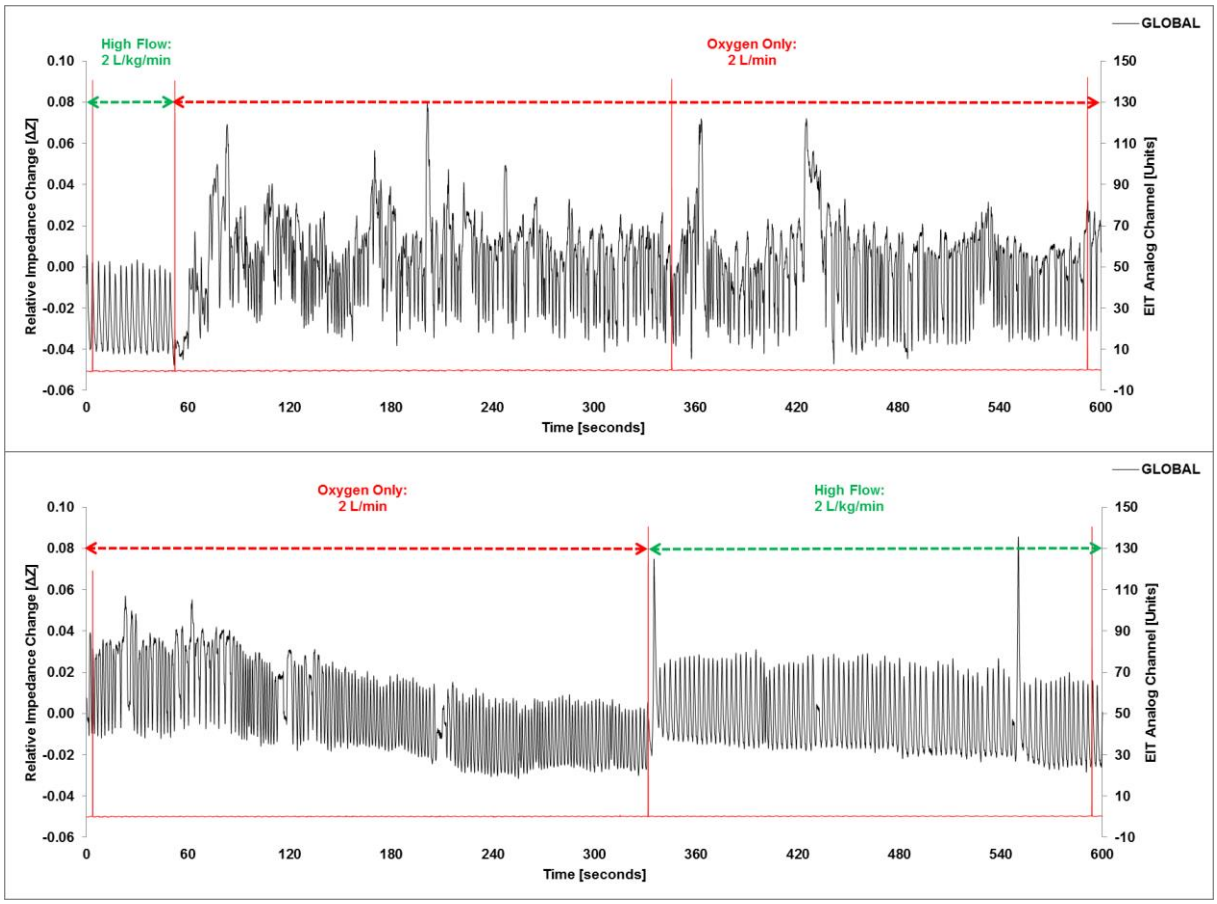

Figure 14: Representative Electrical Impedance Tomography recordings showing the effect of removing and reapplying HFNC therapy. The EIT Analog Channel signal was used as a marker signal to indicate specific changes in HFNC states and provided a means of synchronising these recordings with other signals recorded in LabChart.

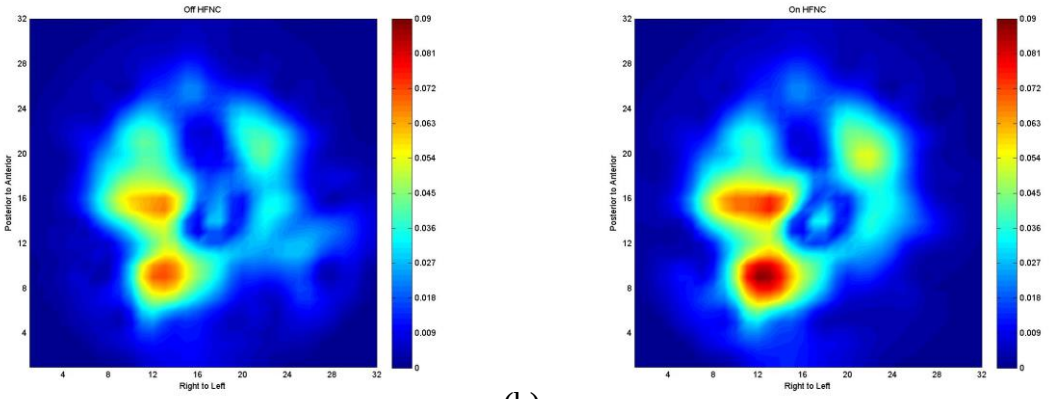

(a) (b)

Figure 15: Representative Electrical Impedance Tomography images showing ventilation distribution (a) off HFNC and (b) on HFNC therapy. Relative impedance changes (ΔZ) increased with the application of HFNC therapy.

4.6 Publications

Significant clinical findings from this program of research were accepted for publication in the journal of Pediatric Pulmonology. The paper, titled "The effect of high flow nasal cannula therapy on the work of breathing in infants with Bronchiolitis", was published online (Epub ahead of print) in mid-2014 before appearing in print in mid-2015 (Pediatric Pulmonology 2015; 50: 713-720) (Pham, O'Malley et al. 2015). A second publication, describing the specific calculation steps for examining TAA using the LLA method in LabChart, is currently in planning. Further work regarding the Edi signal is also in discussion with the investigators of the broader clinical study from which this program of research is based.

5 DISCUSSION

To contextualise the research findings, the results must be discussed in terms of the clinical significance to the broader clinical study, from which this program of research is based. A summary of specific findings, in relation to the clinical WOB scoring component of the broader clinical study, is presented in Appendix A.4.

5.1 WOB Measurements and Assessments

5.1.1 Electrical Activity of the Diaphragm

Since the diaphragm is a muscle whose effort is modulated by the number of activated muscle fibres, a reduction in a signal of the electrical activity of the diaphragm would imply a decrease in oxygen consumption by the respiratory system and the postulated offloading of the diaphragm could be demonstrated with an Edi signal. It is notable that infants with Bronchiolitis showed greater baseline Edi values compared to the group of Cardiac infants, a finding which is consistent with the observed Edi values of patients with respiratory diseases (Emeriaud, Larouche et al. 2014). Overall, infants with Bronchiolitis showed average inspiratory drive values (Edi_{MAX} and Edi_{AMPL}) >25μV off HFNC therapy while Cardiac infants showed values <15μV. Normal values for Edi_{MAX} have been reported to be between 10 and 15μV. It has been demonstrated that changes in the tonic activity of the diaphragm are associated with changes in end-expiratory lung volume (EELV) and that persistent diaphragmatic activity during the expiratory phase helps to regulate EELV (Emeriaud, Beck et al. 2006) (Lopes, Muller et al. 1981). Again, in infants with Bronchiolitis, indicators of the tonic activation of the diaphragm at end-expiration, Edi_{MIN}, were also consistently higher compared to those of the Cardiac infants. As expected, the effect of HFNC on WOB had the greatest overall impact in the group of infants with Bronchiolitis, as measured with Edi. However, it is interesting to note that significant changes were also detectable, off HFNC to on HFNC, in the group of Cardiac infants where the measured values were generally smaller.

5.1.2 Respiratory Inductance Plethysmography

In comparison with Edi, similar changes in the indicators for respiratory drive (RIP_{MAX} and RIP_{AMPL}) and EELV (RIP_{MIN}) were also measured with RIP. However, RIP measurements were only sensitive enough to detect most of the significant changes in the group of infants with Bronchiolitis. In particular, an increase in RIP_{MIN} was congruent with a decrease in Edi_{MIN}, indicating that less work was required for the maintenance of EELV. Bodily responses to the electrical signals emitted from the neural centres, to drive respiration, will

depend on the disease state and mechanics of the respiratory muscles. Unlike infants with Bronchiolitis, Cardiac infants did not require a lot of respiratory support off HFNC. For Cardiac infants, a reduction in WOB was detected with the application of HFNC, but no clinically relevant changes in respiratory support were actuated.

5.1.3 Oesophageal Pressure

An examination of the oesophageal pressure waveforms yielded similar findings to the RIP and Edi measurements. For both groups, the added respiratory support provided by HFNC resulted in a decrease in Poe_{AMPL} which was consistent with the decrease in RIP_{AMPL}. With the onset of inspiration, any observed drop in mediastinal pressure (Poe) without an observed volume change is equivalent to the PEEPi. With HFNC therapy, PEEPi was reduced, indicating the CPAP effect of HFNC in lessening small airway obstruction. However, as with the EELV results between infants with Bronchiolitis and Cardiac infants, changes in PEEPi as well as the traditional WOB measurement, PRP, were only significant for infants with Bronchiolitis. Again, while the Cardiac group showed a slight reduction in WOB, the impact on Poe did not reveal a clinically significant improvement in PEEPi or PRP with the application of HFNC. The PTP(di) is a calculation which considers the effort of the diaphragm. PTP quantifies inspiratory effort, giving a good indication of the energy expenditure of the respiratory muscles and has been used to estimate the metabolic cost of breathing. As was demonstrated with the Edi signal, PTP(di) was able to detect a reduction in WOB for both groups, regardless of the scale of measured values off and on HFNC.

5.1.4 LLA for TAA

An increase in RC_{MIN} and ABD_{MIN} was consistent with an increase in EELV on HFNC. For both groups, a significant increase in RC_{AMPL} with an accompanying decrease in ABD_{AMPL} indicated an increase in respiratory support with less respiratory drive from the diaphragm. These results strengthen and support the previous findings of the Edi, RIP and Poe. However, Cardiac infants showed a better response to HFNC than infants with Bronchiolitis when respiratory distress was examined using the LLA method. Phase angles are elevated in cases of acute upper airway obstruction. Reductions are consistent with changes in the degree of stridor and are accompanied by improvements in inspiratory flows and tidal volumes (Hammer and Eber 2005). However, despite indications of improved respiratory support, the calculated phase angle, θ, was only shown to be significant in the group of Cardiac infants. In these infants, the width of the LLA loop became narrower on HFNC and similar but not

significant changes could be observed in infants with Bronchiolitis. Since changes could be detected in a group without obstructive airway disease (Cardiac infants), the results suggest further investigation in to the adequacy of HFNC delivery rates, particularly for infants with Bronchiolitis, could be needed.

5.2 WOB Measures for HFNC

For this program of research, LabChart-based macro tools were developed to assist clinicians with the analysis of RIP signals using the LLA method. However, for the purposes of bedside WOB assessments, the use of these tools may not be as time effective as the current method of clinical WOB scoring despite greater accuracy of assessment. Studies comparing RIP against PRP found that PRP was a better discriminator of inspiratory load and respiratory support (Hammer and Eber 2005). However, while both methods have been used successfully to measure different descriptors of respiratory effort, the results are still a secondary response to primary respiratory drive. For instance, RIP examines the movement of the chest wall and abdomen, the control of which changes with maturation, and PRP utilises the respiratory rate as part of the calculation, a physiological parameter that also changes with age. By comparison, the strength of the electrical activity of the diaphragm is independent of age, even in infants less than one year of age where there is greater prevalence in the tonic activation of the diaphragm during expiration.

In this study, it was demonstrated that a signal of the electrical activity of the diaphragm was able to detect changes in WOB in infants on HFNC and that the Edi signal had a greater relationship with the measured changes than traditional measures of WOB. Specifically, the measurement of Edi_{MAX}, Edi_{AMPL} and PTP(di) are promising objective measures for the assessment of WOB. Previously, a similar scale of changes to those measured in these values, have been reported in clinically relevant parameters such as the respiratory rate and heart rate, in infants with Bronchiolitis, treated with HFNC therapy (Schibler, Pham et al. 2011). As changes in these parameters correlate well with the degree of WOB observed clinically, they could potentially be used for the titration of flow rates in infants on HFNC. These findings suggest that a "dose finding" study in HFNC could be undertaken using these physiological measurements as determinants of the efficacy of therapy.

5.2.1 Clinical Significance of Research Findings

The physiological effect of HFNC is presumed to be through an offloading of the diaphragm during inspiration with an increased expiratory resistance and accompanying PEEP during

expiration. With the broader clinical study, the work of breathing in infants with Bronchiolitis was effectively reduced with the application of HFNC therapy, at a rate of 2L/kg/min. The results of this study showed a significant reduction in the measured electrical activity of the diaphragm and oesophageal pressure waveforms in these infants. A similar but less prominent effect could also be demonstrated in the control group of Cardiac infants (without airway obstruction). However, while it was expected that infants with Bronchiolitis would show a greater range of significant results across the measured parameters and calculations compared to the group of Cardiac infants, off and on HFNC therapy, this was not always the case. Determining the optimal flow rate for specific patient groups with differing disease pathophysiology is still a topic of debate among clinicians and treating institutions. Patients enrolled in to the broader clinical study were treated with HFNC therapy at a flow rate of 2L/kg/min, in accordance with the clinical guidelines of the MCH PICU. However, for some patients, this level of support may exceed their actual requirements while for patients who do not respond well to HFNC therapy, this level of support may be inadequate, requiring a clinical review for a higher rate of flow. The effect of specific flow rates was not investigated as part of this program of research and further clinical trials are still needed to determine the safety and efficacies of higher flow rates in infants and children.

5.2.2 Future Directions for WOB and HFNC Flow Rate Titration

In other respiratory support modes, it has been reported that neurally triggered breaths reduce trigger delay, improves ventilator response times and may decrease the WOB in children with Bronchiolitis (Clement, Thurman et al. 2011). In particular, the feasibility and benefit of NAVA has been investigated in children with severe Respiratory Syncytial Virus (RSV) related Bronchiolitis where NAVA was found to provide a less aggressive ventilation, requiring lower inspiratory pressures with good results for oxygenation and more comfort for the children (Liet, Dejode et al. 2011). However, mechanical ventilation and other forms of non-invasive ventilation may interfere with the spontaneous breathing pattern in infants because they have strong reflexes that play a large role in the control of breathing (Beck, Tucci et al. 2004). With HFNC therapy, the delivery of flow rates which match the respiratory requirements of the patient on a breath-by-breath basis has yet to be explored and little evidence regarding weaning strategies currently exist (Farley, Hough et al. 2015). Given the nature and sensitivity of the Edi signal in distinguishing WOB and monitoring respiratory drive, independent of age, further research in to the use of an Edi signal as a primary driving mechanism for delivering flow rates for HFNC should be considered for a future study. Of

course, while commercial Edi catheters which can double as a nasogastric tube already exist, making them ideal for use in intensive care, the engineering challenge now would be to incorporate this technology in to existing bedside monitors in accost effective manner, making the Edi signal simple for routine use in infants. In this way, further clinical research may then be conducted to determine whether using and responding to Edi measurements will make a difference to the outcomes for infants requiring HFNC or other forms of respiratory support.

5.3 Limitations

The main aim of the broader clinical study was to examine the impact of HFNC on WOB in infants with Bronchiolitis. However, the study did not specifically address every postulated mechanism of action, which may have contributed to the efficacy of HFNC, as part of the investigation. Instead, the study focused primarily on the response of the muscles involved with respiration, the resultant pressure generated within the chest and changes in physiological observations, with and without the application of HFNC. Several measurement techniques and calculations were used to describe the impact of HFNC on WOB. However, the sensitivity and specificity of these measurement techniques as predictors of clinical outcome were not investigated as part of the broader clinical study. Further, only one flow rate was utilised as part of the investigation, which may not have provided the best result for all study participants.

In this small physiological study, a group of Cardiac infants were used as a control group to demonstrate the effectiveness of HFNC as a respiratory support mode between infants with and without small airways obstruction. It is noted that these Cardiac infants would have experienced some physiological changes following their respective cardiac surgeries, and were not a strict group of representative “healthy” controls for respiratory comparisons per se. However, these Cardiac infants were a demographically homogenous group with minimal respiratory complications, representing the most feasible and accessible cohort for comparison within the broader clinical study. Overall, Cardiac infants showed consistent responses and slight improvements could be shown in some of the measured parameters and calculations for infants studied within this group.

5.4 Conclusion

HFNC therapy, delivered at a rate of 2L/kg/min, is highly effective in reducing WOB in infants with Bronchiolitis and a similar physiological effect could be observed in infants without significant lung disease. Measurements of the electrical activity of the diaphragm provided a useful clinical tool for the objective assessment of WOB and the efficacy of this non-invasive respiratory support mode. By comparison, a signal of the electrical activity of the diaphragm was demonstrated to be more sensitive in the detection of WOB changes than traditional WOB assessment methods utilising oesophageal pressures or RIP. However, for more comprehensive clinical assessments, measurements of oesophageal pressure and RIP may be used in conjunction with the electrical activity of the diaphragm for better establishing a patient's disease state and their response to treatment.

APPENDICES

A.1 Background to Methodology

Given the clinical nature of the study objectives, a collaborative relationship with an established clinical research group was pertinent for the acquisition of relevant data for analysis. In general, clinical research studies require Human Research Ethics Committee (HREC) clearance and Governance approval, sufficient funding, qualified trained staff and dedicated measurement equipment, before any data collection may commence. At the time of project conception, the Paediatric Critical Care Research Group (PCCRG), affiliated with Mater Research, were in the early planning stages of conducting a study with similar objectives, in the Paediatric Intensive Care Unit (PICU) of the Mater Children's Hospital (MCH), South Brisbane. For this program of research, only access to previously collected and non-identifiable human data from the PCCRG was sought for analysis. As such, this program of research was determined to be exempt from full ethical review and the appropriate approvals were sought and granted by the QUT HREC as well as the Mater Health Services (MHS) HREC and Governance authorisation body. To adhere with ethical guidelines, no part of the PCCRG's on-site data collection regime was completed by representatives of QUT. Instead, extensive consultation was given to the PCCRG regarding the data acquisition and data analysis components of their study, and only relevant non-identifiable human data was accessed and analysed for this program of research.

A.1.1 The Clinical High Flow Work of Breathing Study

Prior to the closure of the MCH in November 2014, the PCCRG conducted a prospective interventional trial in PICU - the clinical High Flow Work of Breathing (HFWOB) study - to examine the effect of High Flow Nasal Cannula (HFNC) therapy on the Work of Breathing (WOB) in infants and children with Bronchiolitis. For their study, a group of infants and children with congenital heart disease (CHD) were used as a "control" group to compare differences between a cohort with (Bronchiolitis) small airways obstruction and a (Cardiac) group with no airway obstruction. Inclusion criteria for the Bronchiolitis group were: (i) clinical diagnosis of Bronchiolitis with increased WOB on HFNC therapy, (ii) oxygen requirement on HFNC > 30%, (iii) aged 0-12 months, and (iv) PCR positive for one of the commonly tested respiratory viruses (Influenza A or B, Rhino/Enterovirus). In the Cardiac group, the inclusion criteria were: (i) oxygen requirement post-extubation, (ii) aged 0-12 months, (iii) no clinical signs of increased WOB, and (iv) readiness to be discharged to a

regular paediatric ward. Excluded were infants with an oxygen requirement > 60%, craniofacial malformations, upper airway obstruction and, in Cardiac patients, a clinically diagnosed increased WOB or diagnosed tracheomalacia.

A.1.2 Study Design

Eligible infants in both study groups were to be measured during two states: (a) off HFNC therapy, where 100% humidified and heated oxygen was delivered sub-nasally to maintain SpO_2>92% and then (b) on HFNC therapy, which was delivered at 2L/kg/min. Since all spontaneously breathing infants with Bronchiolitis, admitted to the MCH PICU, were treated with HFNC as per their standard hospital practice, patients enrolled in this group were taken off HFNC for the first set of measurements. Following each change in HFNC state, whether on-off or off-on, a period of 5 minutes was allowed for stabilisation. Data was then recorded for 10 minutes to capture periods of undisturbed regular breathing for analysis.

In accordance with the HFWOB study objectives, a number of physiological waveforms and clinical observations were recorded. These included: a signal of the electrical activity of the diaphragm (Edi); Respiratory Inductance Plethysmography (RIP), oesophageal pressure (Poe), Electrical Impedance Tomography (EIT) and clinical observations such as the respiratory rate, heart rate, fraction of inspired oxygen (FiO_2) and peripheral oxygen saturations (SpO_2). Clinical WOB scoring was also performed by a dedicated senior research nurse for each study infant, off and on HFNC. For this program of research, only relevant subsets of these measurements and observations were examined for performing WOB assessment calculations.

A.1.3 Timeline for Completion

As highlighted in Annual Progress Reports, a number of challenges and difficulties were experienced during this program of research. Specifically, this program of research relied heavily on the accessibility of viable study data from the efforts of the PCCRG, and as such, project progression was highly dependent on the progress of the PCCRG in accomplishing their own clinical work. Consequently, delays and difficulties experienced by the PCCRG with regard to their rate of patient recruitment, accuracy of data collection and documentation, management of staff turnover and funding had an impact on the timing of specific tasks for this program of research. Delays in ethics and research governance approvals from the MHS HREC were also experienced during project set-up. However, these were eventually resolved.

A.2 LabChart Analysis

It may have been simpler to have performed all the required phase angle and other data analysis tasks for this study, using a software package such as MATLAB. However, clinical research studies have limited funding and access to resources and, from a feasibility standpoint, any data acquisition and analysis approach must be translatable to clinical practice. That is, the ideal solution should be one where clinicians can replicate the findings of their study with minimal access to specialist technical expertise which is not readily available outside of a research setting. In light of these specifications, an integrated data analysis solution, developed in LabChart and Microsoft Excel, was the favoured approach for this program of research.

A.2.1 Design Limitations and Restrictions

LabChart has a limit of 32 channels for data acquisition and analysis. In general, available channel calculations are dependent on specific software modules and extensions installed, and only one type of channel calculation may be output to a given channel at any one time. When performing channel calculations, LabChart uses customisable cycle detection methods to identify waveform excursions and treats each cycle period identified as a complete signal for analysis. A separate channel is used to output the result of each channel calculation. The result channel is a "waveform" of values where the cycle length of each value corresponds to the respective cycle period from which the calculated value was obtained. When specific results are compiled for export, channel values corresponding to a specific marker position within each previously detected cycle period are extracted and saved to an internal spreadsheet area (Data Pad). By default, LabChart defines and detects cycle periods peak-to-peak, and uses the first peak as the marker position for data extraction. However, in a clinical context, data is conceptually more meaningful when examined trough-to-trough where the rising edge from the first trough is generally congruent with inspiration. It is noted that even when the appropriate adjustments are made to the cycle detection settings, the manner in which LabChart constructs "result waveforms" and extracts channel values necessitates a carefully considered approach to ensure correct values are extracted for analysis. A series of LabChart macros was developed to perform channel calculations as economically as possible. Further data analysis macros were then developed in Microsoft Excel to complete the required calculations, and to compile and collate the result data for statistical analysis.

A.2.2 Macro Sequences

Four LabChart macros were primarily developed for analysing the signals collected from the clinical HFWOB study, from which this program of research is based, and a broad range of waveform parameters and related calculations were included in the implementation.

The first LabChart macro was designed to determine the basic waveform parameters of the Edi signal and RIP_{SUM} signal. For these signals, the base "Cyclic Measurements" channel function was used to determine: Edi_{MIN}, Edi_{MAX}, Edi_{AMPL}, Edi_{RR}, Edi_{AUC}, RIP_{MIN}, RIP_{MAX}, RIP_{AMPL}, RIP_{RR} and RIP_{AUC}. Additionally, for the RIP_{SUM} signal, the "Peak Analysis" channel function was used to determine RIP_{Ti}, and RIP_{Ttot}, and channel arithmetic used to determine $RIP_{Ti/Ttot}$. The marker position for data extraction was the start point of each detected cycle.

The second LabChart macro was designed to aid in the calculation of phase angles using the LLA method. To adequately examine the relationship between the RC and ABD signals, a waveform of unit spikes, based on a system definition of the start of inspiration ($RIP_{SUM(InspUnitSpikes)}$), was generated and used to identify cycle periods for analysis. A combination of "Cyclic Measurements" and arithmetic channel calculations were then used to determine: RC_{MAX}, RC_{MIN}, ABD_{MAX}, and ABD_{MIN} as well as the ABD values where RC crosses zero in the LLA loops. A further sequence of arithmetic and "Cyclic Measurements" channel calculations were then performed to determine: the ABD loop excursion when RC is zero (m), the maximum ABD loop excursion (s), a phase angle ($\theta = \arcsin(m/s)$) between 0-90 degrees, and values for Slope Direction and Loop Rotation. The marker position for data extraction was the peak of each detected RIP_{SUM} cycle. To determine a clinically meaningful phase angle value, expressed between -180 to 180 degrees, the final phase angle calculation was performed during the data collation process using an Excel VBA Macro.

The third LabChart macro was designed to determine the basic waveform parameters of the pre-processed EIT signals and Poe signal as well as a limited number of equivalent parameters for the RIP_{SUM}, where available channels permitted. For the pre-processed EIT signals, the base "Cyclic Measurements" channel function was used to determine: $EIT_{GLOBAL\ (AMPL)}$, $EIT_{GLOBAL\ (MAX)}$, $EIT_{GLOBAL\ (MIN)}$, $EIT_{ANTERIOR\ (APML)}$, $EIT_{ANTERIOR\ (MAX)}$, $EIT_{ANTERIOR\ (MIN)}$, $EIT_{POSTERIOR\ (AMPL)}$, $EIT_{POSTERIOR\ (MAX)}$, and $EIT_{POSTERIOR\ (MIN)}$. The marker position for data extraction was the start point of each detected cycle. For the RIP_{SUM} signal, the "Peak Analysis" channel function was used to determine: Baseline (RIP_{MIN}), APeak (RIP_{MAX}), Height (RIP_{AMPL}), TimeToPeak (RIP_{Ti}) and Width (RIP_{Ttot}), and channel arithmetic used to determine $RIP_{Ti/Ttot}$. For the Poe signal, a $RIP_{SUM(InspUnitSpikes)}$ signal (as described in the

second LabChart macro) was generated and applied before the base "Cyclic Measurements" channel function could be used to determine Poe_{MAX} and Poe_{MIN}, and channel arithmetic used to determine Poe_{APML}. With the RIP_{SUM} and Poe signals, the marker position for data extraction was the peak of each detected RIP_{SUM} cycle.

Through specific examination of the RIP_{SUM} and Poe signals, the fourth LabChart macro was designed to perform related calculations for traditional measures of WOB: PRP, PTP(di) and PEEPi. As with the second LabChart macro, a $RIP_{SUM(InspUnitSpikes)}$ signal was generated and used to identify cycle periods for analysis, and a corresponding waveform of the inspiratory duty cycle was also generated and used specifically in the calculation for PTP(di). Following the application of the $RIP_{SUM(InspUnitSpikes)}$ signal, the base "Cyclic Measurements" channel function was used to determine: the respiratory rate (RIP_{RR}), Poe_{MIN} and Poe_{MAX}, and channel arithmetic used to determine Poe_{AMPL}. A sequence of "Cyclic Measurements" and arithmetic operations were then used to determine: PEEPi, PRP and PTP(di), including $\int Poe_{INSP}$ for each breath. The marker position for data extraction was the peak of each detected RIP_{SUM} cycle.

A.2.3 Example LabChart Waveform Recordings

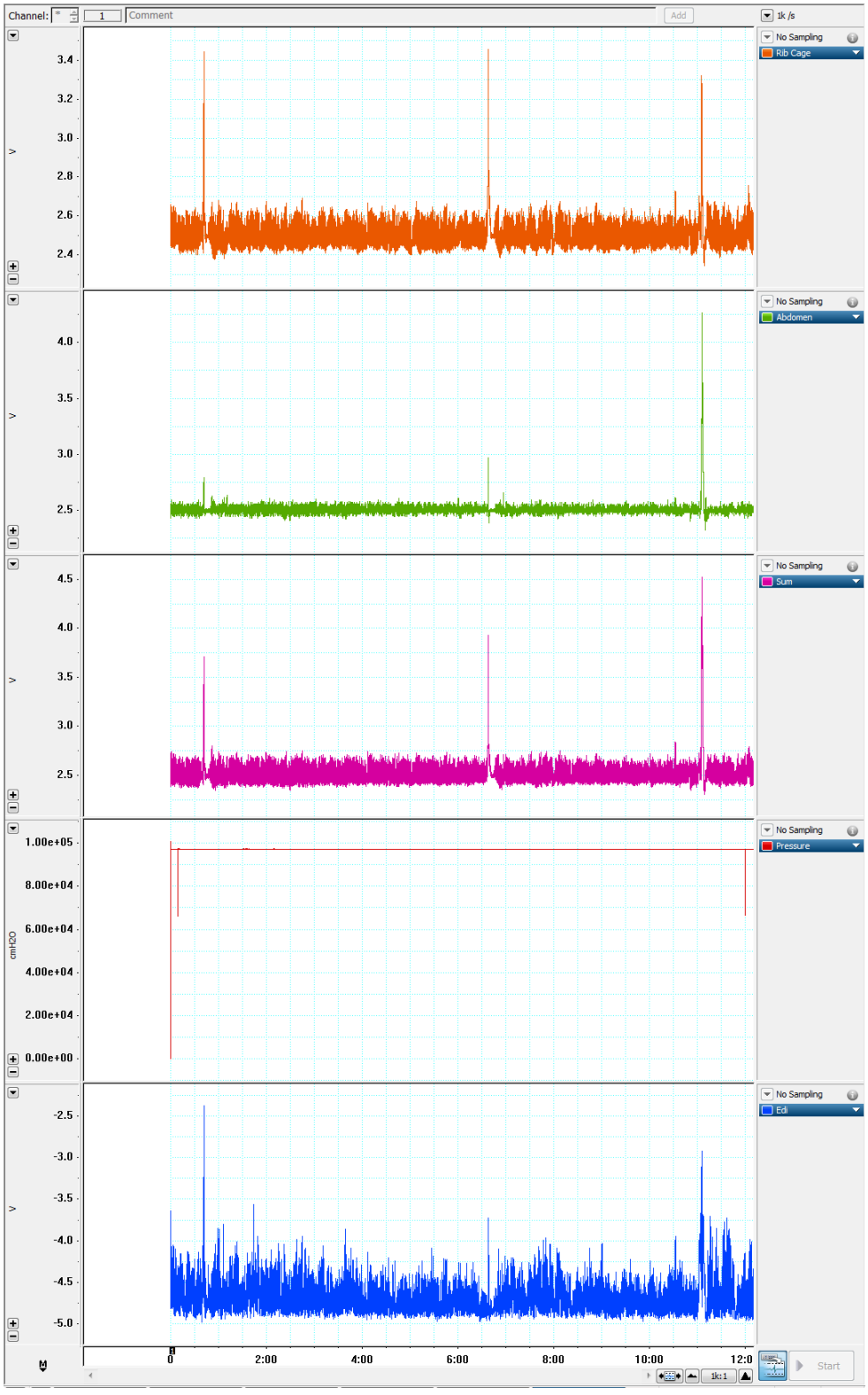

Figure 16: Representative LabChart recording of the RC, ABD, RIP_{SUM} and Edi signals of an infant on HFNC delivered at 2L/kg/min. In this example, no Poe signal was recorded (red line in the fourth channel). Instead, a trigger signal was attached to the Poe Channel to aid in later analysis.

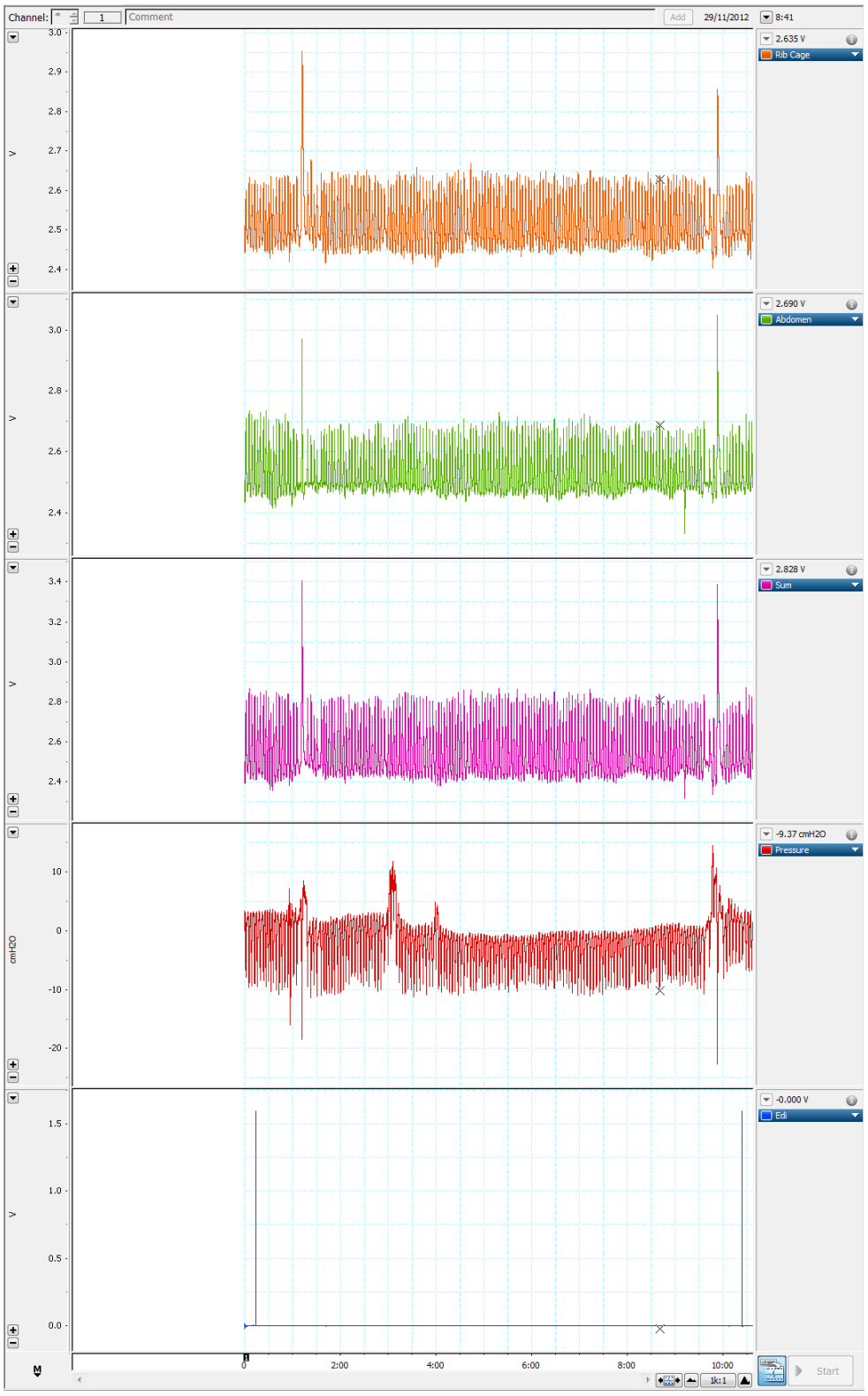

Figure 17: Representative LabChart recording of the RC, ABD, RIP_{SUM} and Poe signals of an infant on HFNC delivered at 2L/kg/min. In this example, no Edi signal was recorded (blue line in the fifth channel). Instead, a trigger signal was attached to the Edi Channel to aid in later analysis.

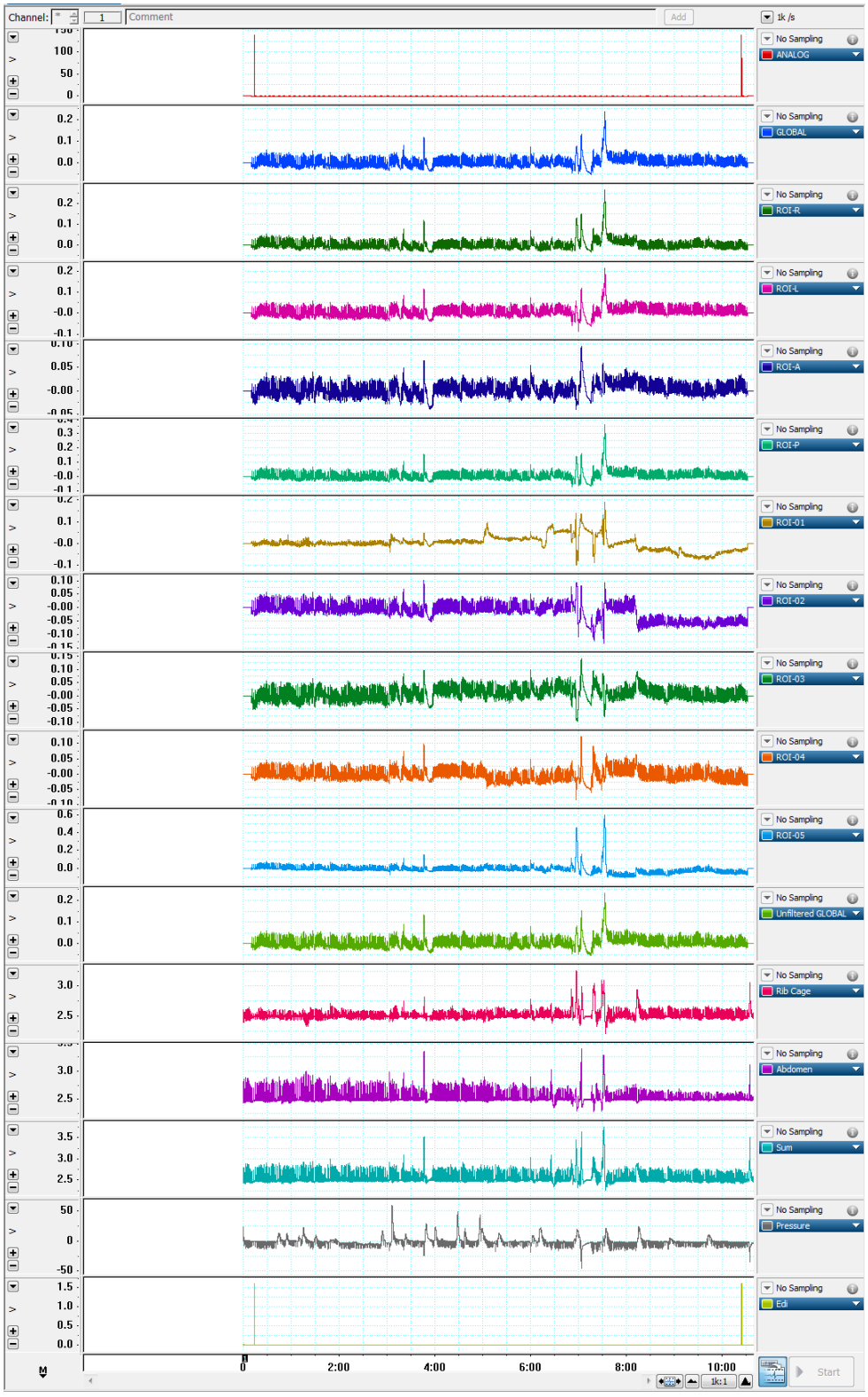

Figure 18: Representative example of synchronised pre-processed EIT signals inserted in to a LabChart file.

A.2.4 Example LabChart Macro Recordings

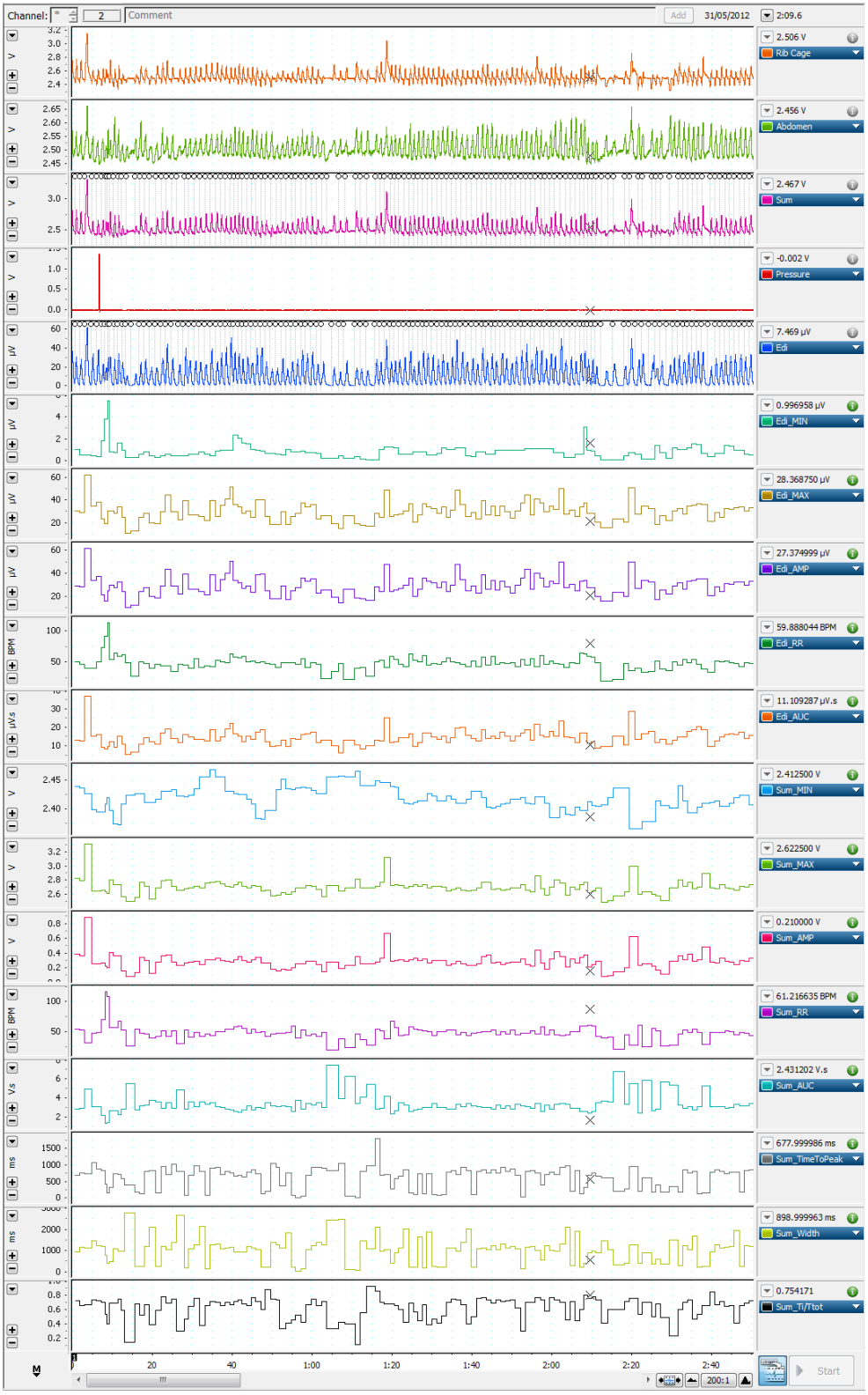

Figure 19: Representative result waveforms from the first LabChart Macro (Macro I: Edi and RIP_{SUM} Analysis).

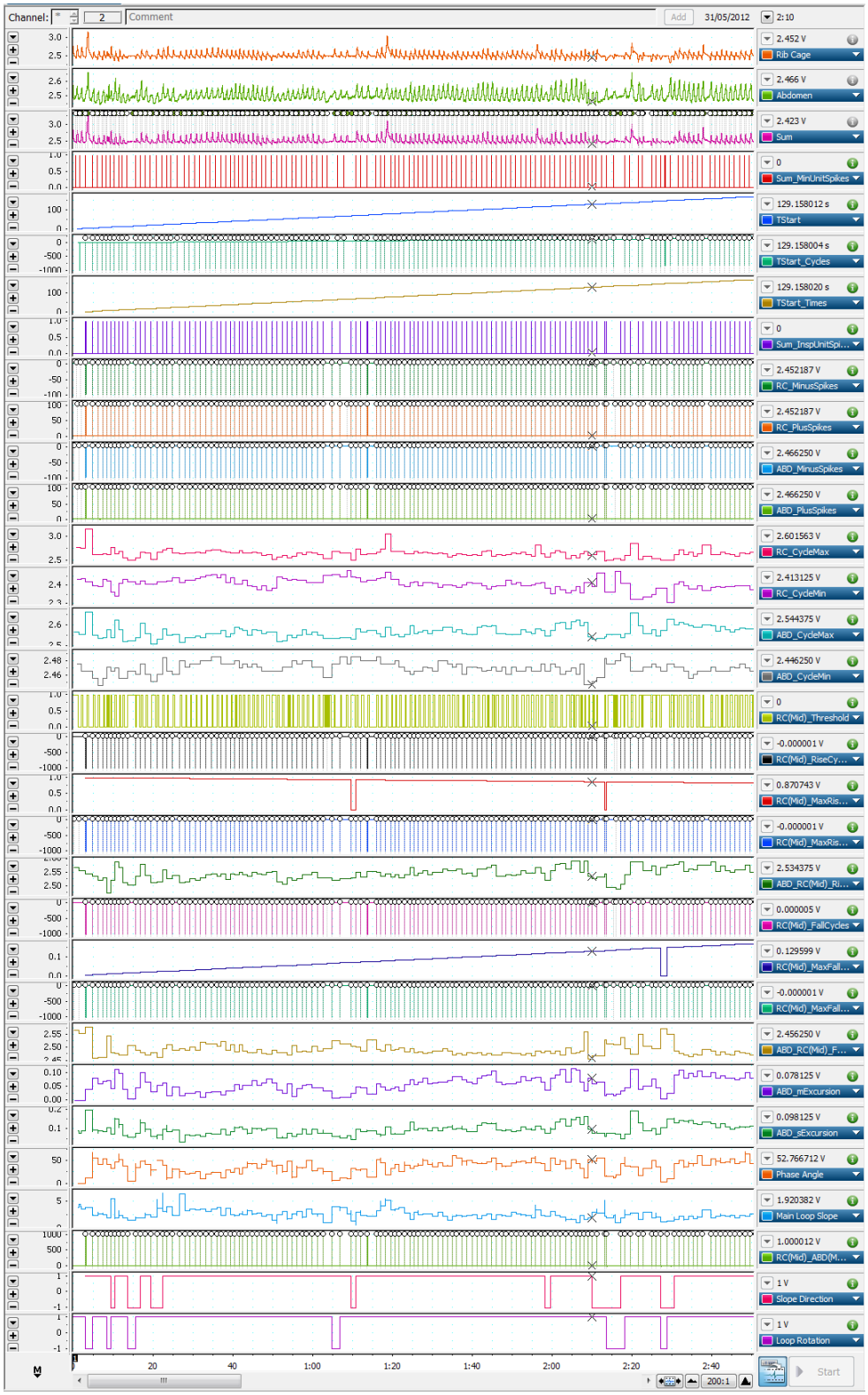

Figure 20: Representative result waveforms from the second LabChart Macro (Macro II: LLA Analysis).

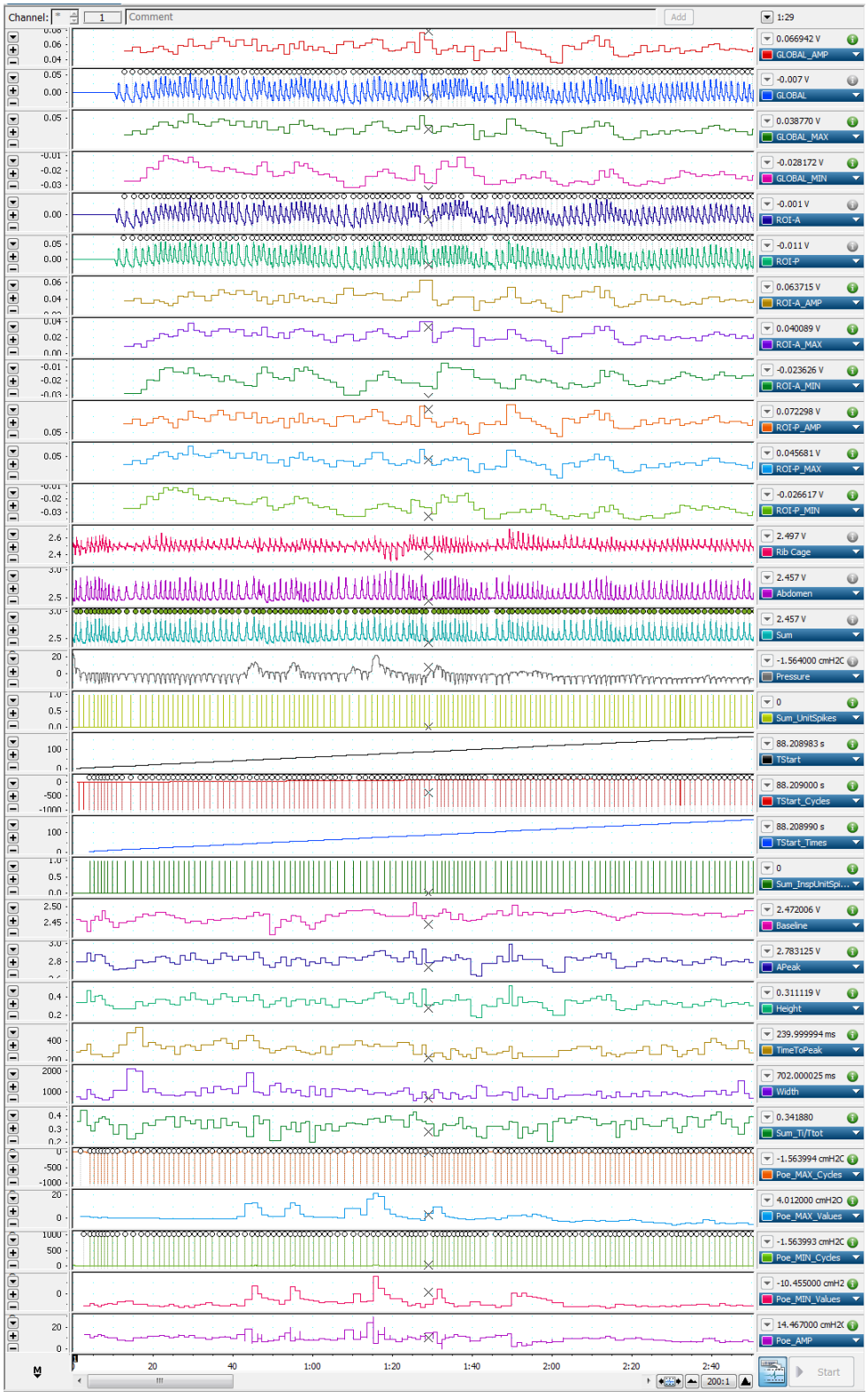

Figure 21: Representative result waveforms from the third LabChart Macro (Macro III: EIT, Poe and RIP_{SUM} Analysis).

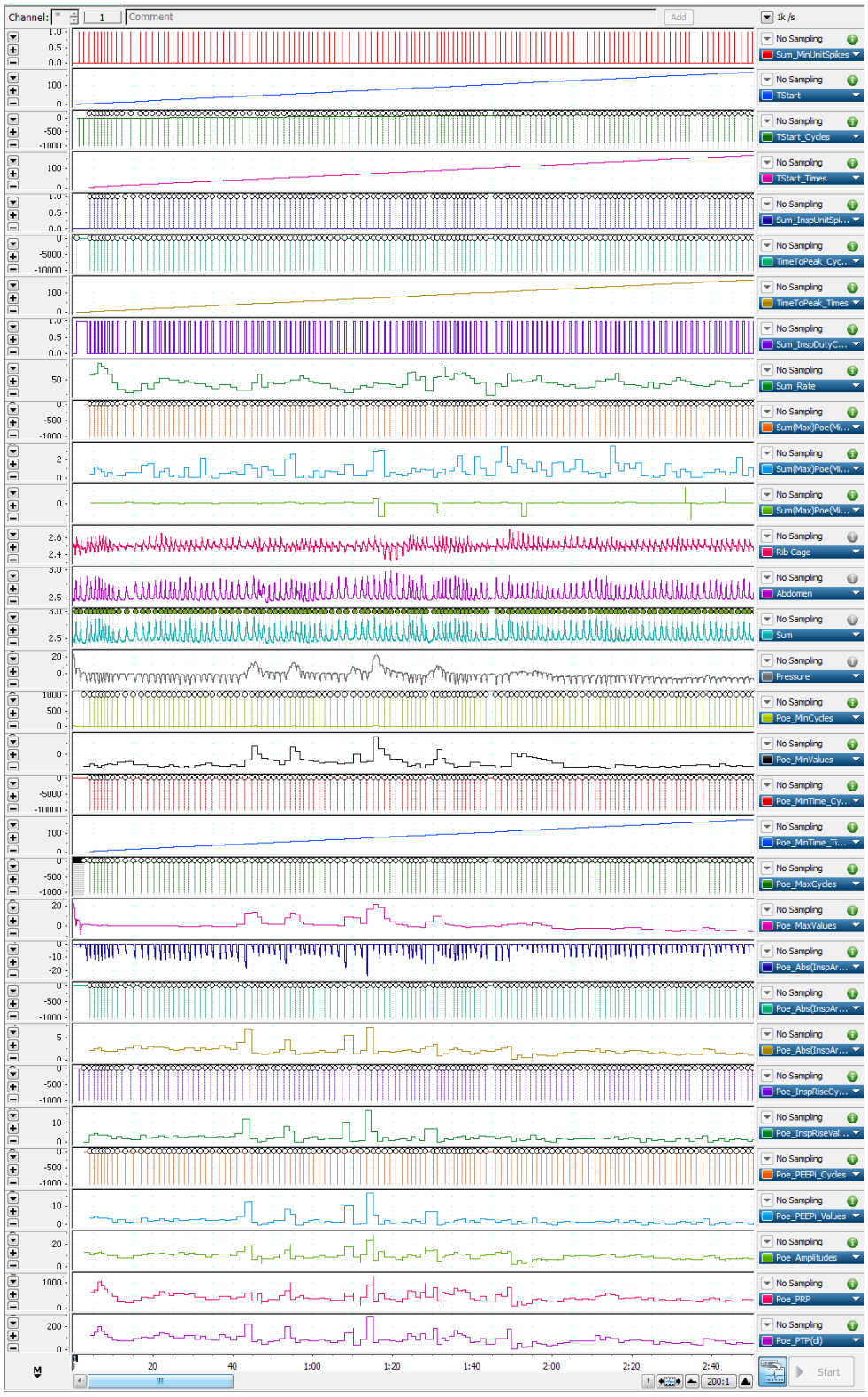

Figure 22: Representative result waveforms from the fourth LabChart Macro (Macro IV: RIP_{SUM}, Poe, PRP, PTP(di) and PEEPi Analysis).

A.3 EIT Results using the EIT Data Analyser

Table 6: Mean values and absolute mean changes in the Electrical Impedance Tomography measurements taken for infants with Bronchiolitis and Cardiac infants, off and on HFNC. These results were obtained using the PCCRG's standardised EIT data analysis protocol (originally written by me) where calculations were performed separately from the main LabChart analysis. Paired samples t-Tests were used to compare HFNC states within groups (*). An ANOVA was used to compare mean changes between groups (^). A p-value of <0.05 was considered to be statistically significant.

	Bronchiolitis		Cardiac Infants		Between Groups	
	Off HFNC *Mean*	On HFNC *Mean*	Off HFNC *Mean*	On HFNC *Mean*	Bronchiolitis $\lvert\Delta$ *Mean*$\rvert$	Cardiac $\lvert\Delta$ *Mean*$\rvert$
EEL_G [ΔZ]	-0.016199	0.004180	-0.004803	0.004889	0.020379	0.009692
p-value	0.062		0.140		0.595	
EEL_R [ΔZ]	-0.026744	0.006589	-0.001334	0.007410	0.033333	0.008744
p-value	0.008*		0.291		0.347	
EEL_L [ΔZ]	-0.011165	-0.000471	-0.002559	0.009087	0.010694	0.011646
p-value	0.262		0.070		0.552	
EEL_A [ΔZ]	-0.015730	0.010048	-0.021009	-0.004943	0.025778	0.016066
p-value	0.072		0.064		0.433	
EEL_P [ΔZ]	-0.022566	-0.003599	0.008033	0.016832	0.018967	0.008799
p-value	0.119		0.276		0.091	
$AMPL_G$ [ΔZ]	0.031761	0.026093	0.040290	0.038937	0.005668	0.001353
p-value	0.032*		0.319		0.076	
$AMPL_R$ [ΔZ]	0.035737	0.028537	0.043786	0.042339	0.007200	0.001447
p-value	0.031*		0.317		0.159	
$AMPL_L$ [ΔZ]	0.029265	0.024522	0.036353	0.035406	0.004743	0.000947
p-value	0.055		0.377		0.133	
$AMPL_A$ [ΔZ]	0.028403	0.023552	0.038938	0.037032	0.004851	0.001906
p-value	0.062		0.265		0.065	
$AMPL_P$ [ΔZ]	0.041174	0.032525	0.041632	0.039630	0.008649	0.002002
p-value	0.012*		0.279		0.562	
$ALPHA_R$ [°]	10.351	8.982	5.207	2.872	1.369	2.335
p-value	0.304		0.145		0.064	
$ALPHA_L$ [°]	-8.967	-10.398	-6.813	-5.047	1.431	1.766
p-value	0.322		0.151		0.320	

$ALPHA_A$ [°]	-13.209	-11.291	-3.636	-3.885	1.918	0.249
p-value	0.280		0.448		0.006^	
$ALPHA_P$ [°]	11.807	9.249	3.036	-0.556	2.558	3.592
p-value	0.075		0.077		0.013^	
GC_{GLOBAL} [%]	47.523	45.293	48.189	48.251	2.230	0.063
p-value	0.039*		0.477		0.060	
GC_{RIGHT} [%]	45.773	44.163	47.430	47.546	1.610	0.116
p-value	0.020*		0.465		0.029^	
GC_{LEFT} [%]	47.481	46.400	47.573	48.758	1.081	1.185
p-value	0.246		0.213		0.349	
FI_R [Units]	0.893	0.881	0.949	0.948	0.012	0.001
p-value	0.319		0.459		0.050^	
FI_L [Units]	1.271	1.342	1.302	1.035	0.071	0.267
p-value	0.181		0.160		0.084	
FI_A [Units]	1.252	1.223	1.078	1.034	0.029	0.044
p-value	0.319		0.021*		0.005^	
FI_P [Units]	0.858	0.868	0.974	1.001	0.010	0.027
p-value	0.226		0.041*		0.018^	
GI INDEX [0-1]	0.422	0.440	0.422	0.420	0.018	0.002
p-value	0.122		0.467		0.538	

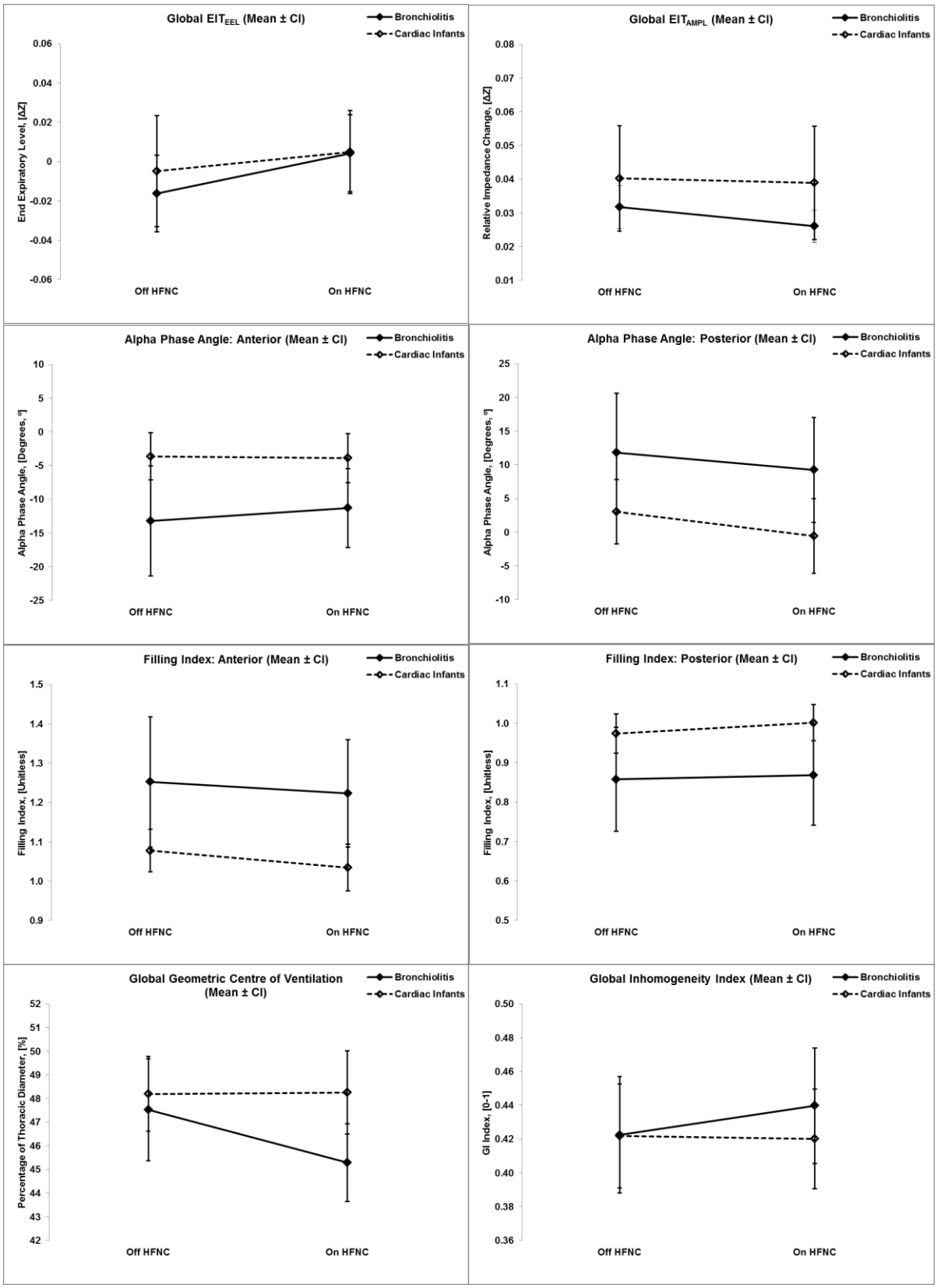

Figure 23: Mean values of the Electrical Impedance Tomography calculations for infants with Bronchiolitis and Cardiac infants, off and on HFNC. Mean and 95% confidence intervals are shown.

A.4 Clinical Findings

To facilitate the interpretation of results, collected from the clinical HFWOB study, non-identifiable human data was analysed in collaboration with the PCCRG. The main results of this collaborative analysis, which are relevant to this program of research, are described in main body of this thesis. However, specific findings in relation to the clinical WOB scoring component, for both the Bronchiolitis (treatment) and Cardiac (control) groups, are presented here.

A.4.1 The Clinical HFWOB Study

Between May 2012 and February 2013, the PCCRG enrolled infants in to their HFWOB study with 14 recruited in to the Bronchiolitis (treatment) group and 14 recruited in to the Cardiac (control) group. However, only 12 infants from each group had recordings that were technically sufficient for analysis. This was generally attributed to the unsettledness of the infants following the insertion and adjustment of the Edi catheter, which made it difficult to maintain good signal quality. Regarding the cohorts studied, infants with Bronchiolitis were 56 days old [44, 72] with a body weight of 5.3 kg [4.6, 5.7] and Cardiac infants were 55 days old [18, 96] and with a body weight of 3.8 kg [3.3, 4.6] (median and interquartile range). Two of the infants with Bronchiolitis were ex-preterm without chronic lung disease and of the Cardiac infants, 9 were post bypass cases and 5 non bypass cases. The respiratory rate (RR) in infants with Bronchiolitis dropped from 60 breaths/min [54, 66] off HFNC to 54 breaths/min [48, 60] on HFNC (mean and 95% CI, p=0.004) and in Cardiac infants, the RR changed from 48 breaths/min [36, 60] to 41 breaths/min [32, 50] (mean and 95% CI, p=ns).

A.4.2 Clinical WOB Scoring: Results

The standard clinical scoring system used to assess the WOB and degree of respiratory distress in MCH PICU (Table 7), is subjective and based on the clinical experience of the observer. It was not specifically developed for, nor has it been validated for using with HFNC. However, for consistency, standardised WOB assessments for each patient enrolled in the clinical HFWOB study were performed by the same experienced Research Nurse, off and on HFNC. To represent these qualitative assessments graphically, WOB categories were assigned to a numerical scale (from 0 to 5, where 0 is none and 5 is severe), and plotted (Figure 24).

Table 7: Respiratory assessment guidelines, as used by clinical staff at the MCH PICU, include observable WOB criteria. Standard assessments are objective and based on the clinical experience of the observer.

Mild	Moderate	Severe
• RR within age parameter • Minimal accessory muscle use (slight ST/IC recession) • O_2 sats > 93% on RA • Normal colour, behaviour	• RR increased for age group • Accessory muscle use has increased (retractions also) • O_2 sats < 93%, supportive oxygen required • Colour pale/slightly mottled • Reduced feeding • Irritability, tiredness	• RR markedly increased for age group (tachypnoeic++) • Full use of all accessory muscles, marked WOB • Grunting & head bobbing • Apnoeas • O_2 sats continually < 93% despite oxygen support • Colour pale >> dusty • Refusal to feed/oral intake • Lethargy >> fatiguing • Diaphoresis • Skin temp cool • Increased CO_2 on Blood Gas

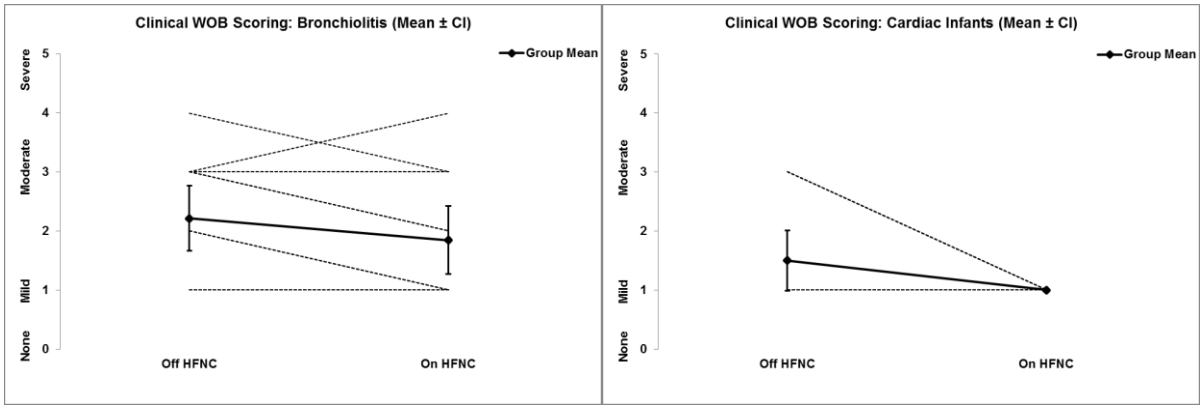

Figure 24: Individual WOB category assessments for infants with Bronchiolitis and Cardiac infants, off and on HFNC. The group means and 95% confidence intervals are also shown.

Overall, the clinical scoring method for assessing WOB and respiratory distress was able to show a slight decrease in severity from off HFNC to on HFNC therapy for each group. However, within each group, particularly for infants with Bronchiolitis, the individual results and the observed parameters used to obtain them (RR and SpO_2), demonstrated a large degree of variability across the broadly defined categories of WOB (Figure 25).

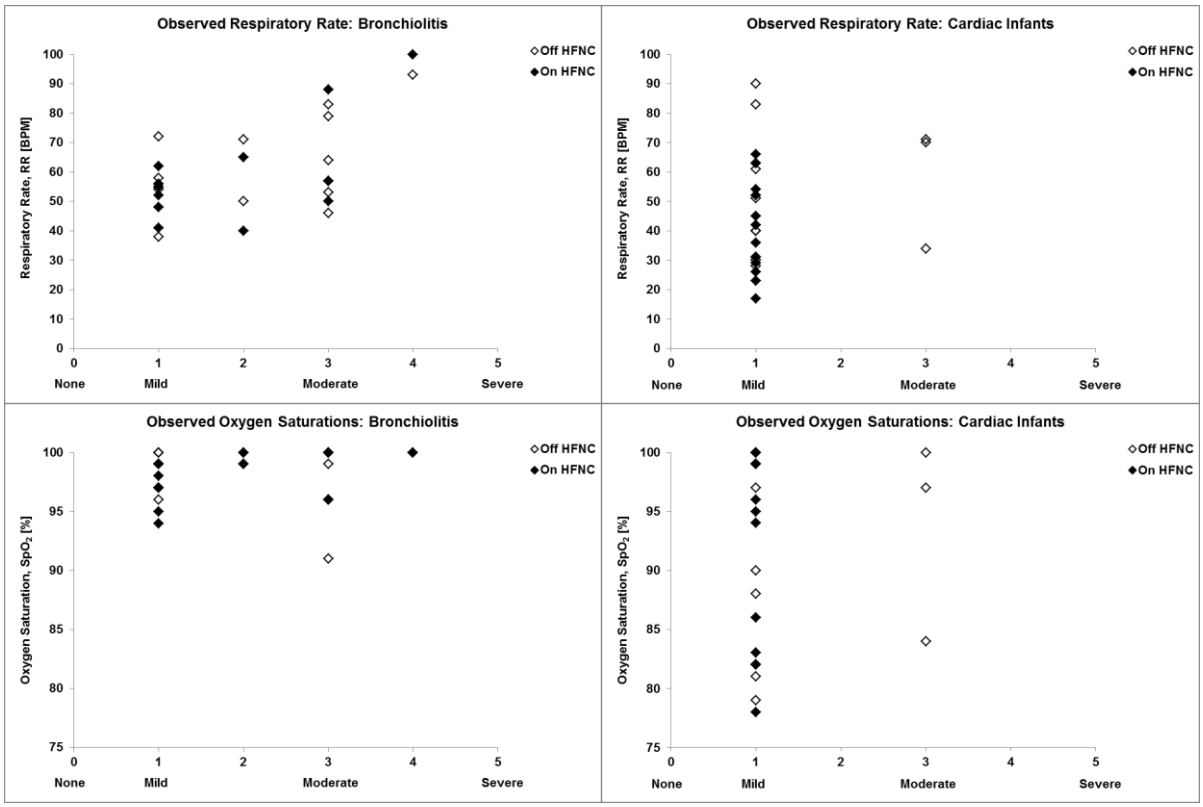

Figure 25: Observed values of respiratory rate and oxygen saturation, used in the clinical scoring method of assessing WOB and respiratory distress, for infants with Bronchiolitis and Cardiac infants, off and on HFNC.

A.4.3 Clinical WOB Scoring: Discussion

Clinical WOB scoring utilises the RR as one of the determinants for WOB categories which, for the clinical HFWOB study, were conducted by the same experienced Research Nurse for each patient, off and on HFNC. In infants with Bronchiolitis, the RR dropped significantly from off HFNC to on HFNC and a similar though not significant drop was also measured in the group of Cardiac infants. While these assessments were able to reflect an overall reduction in the WOB for both groups, little distinction could be made regarding the spread of individually observed RR values between HFNC states when examined by WOB category. Similarly, an overlap of RR values was also observed for the Cardiac infants and in the spread of individual oxygen saturation values between HFNC states for both groups. Clinical WOB scoring may be performed quickly by the bedside. However, even with measurable parameters such as the RR and oxygen saturation and the expertise of a consistent and experienced observer, there is a still a degree of variability to the results that demands caution from the use of clinical scoring systems.

REFERENCES

Alexander, J., J. Millar, A. Slater and J. Woosley (2014). Report of the Australian and New Zealand Paediatric Intensive Care Registry 2013. Melbourne, The Australian and New Zealand Intensive Care Society.

Banner, M. J., R. R. Kirby, A. Gabrielli, P. B. Blanch and A. J. Layon (1994). "Partially and totally unloading respiratory muscles based on real-time measurements of work of breathing. A clinical approach." Chest **106**(6): 1835-1842.

Baudin, F., R. Pouyau, F. Cour-Andlauer, J. Berthiller, D. Robert and E. Javouhey (2015). "Neurally adjusted ventilator assist (NAVA) reduces asynchrony during non-invasive ventilation for severe bronchiolitis." Pediatric Pulmonology **50**(12): 1320-1327.

Beck, J., G. Emeriaud, Y. Liu and C. Sinderby (2015). "Neurally Adjusted Ventilatory Assist (NAVA) in children: a systematic review." Minerva Anestesiologica: [Epub ahead of print].

Beck, J., C. Sinderby, L. Lindstrom and A. Grassino (1998). "Effects of lung volume on diaphragm EMG signal strength during voluntary contractions." Journal Of Applied Physiology **85**(3): 1123-1134.

Beck, J., M. Tucci, G. Emeriaud, J. Lacroix and C. Sinderby (2004). "Prolonged neural expiratory time induced by mechanical ventilation in infants." Pediatric Research **55**(5): 747-754.

Bell, N., C. L. Hutchinson, T. C. Green, E. Rogan, K. J. Bein and M. M. Dinh (2015). "Randomised control trial of humidified high flow nasal cannulae versus standard oxygen in the emergency department." Emergency Medicine Australasia: [Epub ahead of print].

Bellani, G., A. Coppadoro, N. Patroniti, M. Turella, S. Arrigoni Marocco, G. Grasselli, T. Mauri and A. Pesenti (2014). "Clinical assessment of auto-positive end-expiratory pressure by diaphragmatic electrical activity during pressure support and neurally adjusted ventilatory assist." Anesthesiology **121**(3): 563-571.

Bellani, G., T. Mauri, A. Coppadoro, G. Grasselli, N. Patroniti, S. Spadaro, V. Sala, G. Foti and A. Pesenti (2013). "Estimation of patient's inspiratory effort from the electrical activity of the diaphragm." Critical Care Medicine **41**(6): 1483-1491.

Brochard, L., G. S. Martin, L. Blanch, P. Pelosi, F. J. Belda, A. Jubran, L. Gattinoni, J. Mancebo, V. M. Ranieri, J.-C. M. Richard, D. Gommers, A. Vieillard-Baron, A. Pesenti, S. Jaber, O. Stenqvist, J.-L. Vincent, a. Sahlgrenska, s. f. a. b. o. o. A. f. a. o. i. Institutionen för kliniska vetenskaper, A. Sahlgrenska, G. University of, u. Göteborgs, S. f. A. B. Institute of Clinical Sciences, A. Orthopaedics. Department of and c. Intensive (2012). "Clinical review: Respiratory monitoring in the ICU - a consensus of 16." Critical Care **16**(2): 219.

Bueno Campaña, M., J. Olivares Ortiz, C. Notario Muñoz, M. Rupérez Lucas, A. Fernández Rincón, O. Patiño Hernández and C. Calvo Rey (2014). "High flow therapy versus hypertonic saline in bronchiolitis: randomised controlled trial." Archives Of Disease In Childhood **99**(6): 511-515.

Cala, S. J., P. Wilcox, J. Edyvean, M. Rynn and L. A. Engel (1991). "Oxygen cost of inspiratory loading: resistive vs. elastic." Journal Of Applied Physiology **70**(5): 1983-1990.

Castro-Rodriguez, J. A., C. E. Rodriguez-Martinez and M. P. Sossa-Briceño (2015). "Principal findings of systematic reviews for the management of acute bronchiolitis in children." Paediatric Respiratory Reviews **16**(4): 267-275.

Chang, G. Y., C. A. Cox and T. H. Shaffer (2011). "Nasal cannula, CPAP, and high-flow nasal cannula: effect of flow on temperature, humidity, pressure, and resistance." Biomedical Instrumentation & Technology **45**(1): 69-74.

Clement, K. C., T. L. Thurman, S. J. Holt and M. J. Heulitt (2011). "Neurally triggered breaths reduce trigger delay and improve ventilator response times in ventilated infants with bronchiolitis." Intensive Care Medicine **37**(11): 1826-1832.

Collett, P. W. and L. A. Engel (1986). "Influence of lung volume on oxygen cost of resistive breathing." Journal Of Applied Physiology **61**(1): 16-24.

Collett, P. W., C. Perry and L. A. Engel (1985). "Pressure-time product, flow, and oxygen cost of resistive breathing in humans." Journal Of Applied Physiology **58**(4): 1263-1272.

Courtney, S. E., Z. H. Aghai, J. G. Saslow, K. H. Pyon and R. H. Habib (2003). "Changes in lung volume and work of breathing: A comparison of two variable-flow nasal continuous positive airway pressure devices in very low birth weight infants." Pediatric Pulmonology **36**(3): 248-252.

Da Dalt, L., S. Bressan, F. Martinolli, G. Perilongo and E. Baraldi (2013). "Treatment of bronchiolitis: state of the art." Early Human Development **89 Suppl 1**: S31-36.

Dani, C., S. Pratesi, C. Migliori and G. Bertini (2009). "High flow nasal cannula therapy as respiratory support in the preterm infant." Pediatric Pulmonology **44**(7): 629-634.

de Jongh, B. E., R. Locke, A. Mackley, J. Emberger, D. Bostick, J. Stefano, E. Rodriguez and T. H. Shaffer (2014). "Work of breathing indices in infants with respiratory insufficiency receiving high-flow nasal cannula and nasal continuous positive airway pressure." Journal Of Perinatology **34**(1): 27-32.

de la Oliva, P., C. Schüffelmann, A. Gómez-Zamora, J. Villar and R. M. Kacmarek (2012). "Asynchrony, neural drive, ventilatory variability and COMFORT: NAVA versus pressure support in pediatric patients. A non-randomized cross-over trial." Intensive Care Medicine **38**(5): 838-846.

Diehl, J. L., A. Mercat, E. Guerot, F. Aissa, J. L. Teboul, C. Richard and J. Labrousse (2003). "Helium/oxygen mixture reduces the work of breathing at the end of the weaning process in patients with severe chronic obstructive pulmonary disease." Critical Care Medicine **31**(5): 1415-1420.

Ducharme-Crevier, L., G. Du Pont-Thibodeau and G. Emeriaud (2013). "Interest of monitoring diaphragmatic electrical activity in the pediatric intensive care unit." Critical Care Research And Practice **2013**: 384210.

Dysart, K., T. L. Miller, M. R. Wolfson and T. H. Shaffer (2009). "Research in high flow therapy: Mechanisms of action." Respiratory Medicine **103**(10): 1400-1405.

Emeriaud, G., J. Beck, M. Tucci, J. Lacroix and C. Sinderby (2006). "Diaphragm electrical activity during expiration in mechanically ventilated infants." Pediatric Research **59**(5): 705-710.

Emeriaud, G., A. Larouche, L. Ducharme-Crevier, E. Massicotte, O. Fléchelles, A.-A. Pellerin-Leblanc, S. Morneau, J. Beck and P. Jouvet (2014). "Evolution of inspiratory diaphragm activity in children over the course of the PICU stay." Intensive Care Medicine **40**(11): 1718-1726.

Fallot, A. (2005). "Respiratory distress." Pediatric Annals **34**(11): 885-891.

Farley, R. C., J. L. Hough and L. A. Jardine (2015). "Strategies for the discontinuation of humidified high flow nasal cannula (HHFNC) in preterm infants." The Cochrane Database Of Systematic Reviews **6**: CD011079.

Fauroux, B., N. Hart, Y. M. Luo, S. MacNeill, J. Moxham, F. Lofaso and M. I. Polkey (2003). "Measurement of diaphragm loading during pressure support ventilation." Intensive Care Medicine **29**(11): 1960-1966.

Fernández, J., D. Miguelena, H. Mulett, J. Godoy and F. Martinón-Torres (2013). "Adaptive support ventilation: State of the art review." Indian Journal of Critical Care Medicine **17**(1): 16-22.

Frerichs, I., J. Hinz, P. Herrmann, G. Weisser, G. Hahn, T. Dudykevych, M. Quintel and G. Hellige (2002). "Detection of local lung air content by electrical impedance tomography compared with electron beam CT." Journal Of Applied Physiology **93**(2): 660-666.

Frerichs, I., H. Schiffmann, R. Oehler, T. Dudykevych, G. Hahn, J. Hinz and G. Hellige (2003). "Distribution of lung ventilation in spontaneously breathing neonates lying in different body positions." Intensive Care Medicine **29**(5): 787-794.

Gemke, R. J. B. J., J. G. van Keulen and K. H. Polderman (2005). "Reliability of PRISM and PIM scores in paediatric intensive care." Archives Of Disease In Childhood **90**(2): 211-214.

Goldman, M. D., G. Grimby and J. Mead (1976). "Mechanical work of breathing derived from rib cage and abdominal V-P partitioning." Journal Of Applied Physiology **41**(5 Pt. 1): 752-763.

Gottfried, S. B., S. Friberg, P. Navalesi, Y. Skrobik, N. Comtois, L. Lindström, C. Sinderby and J. Beck (1999). "Neural control of mechanical ventilation in respiratory failure." Nature Medicine **5**(12): 1433-1436.

Grant, C. A., T. Pham, J. Hough, T. Riedel, C. Stocker and A. Schibler (2011). "Measurement of ventilation and cardiac related impedance changes with electrical impedance tomography." Critical Care **15**(1): R37.

Greenspan, J. S., M. R. Wolfson and T. H. Shaffer (1991). "Airway responsiveness to low inspired gas temperature in preterm neonates." The Journal Of Pediatrics **118**(3): 443-445.

Groves, N. and A. Tobin (2007). "High flow nasal oxygen generates positive airway pressure in adult volunteers." Australian Critical Care **20**(4): 126-131.

Guslits, B. G., S. E. Gaston, M. H. Bryan, S. J. England and A. C. Bryan (1987). "Diaphragmatic work of breathing in premature human infants." Journal Of Applied Physiology **62**(4): 1410-1415.

Hammer, J. and C. J. L. Newth (2009). "Assessment of thoraco-abdominal asynchrony." Paediatric Respiratory Reviews **10**(2): 75-80.

Hammer, J. r. and E. Eber (2005). Paediatric Pulmonary Function Testing. New York;Basel;, Karger.

Hasan, R. A. and R. H. Habib (2011). "Effects of flow rate and airleak at the nares and mouth opening on positive distending pressure delivery using commercially available high-flow nasal cannula systems: a lung model study." Pediatric Critical Care Medicine **12**(1): e29-33.

Hough, J. L., L. Johnston, S. G. Brauer, P. G. Woodgate, T. M. Pham and A. Schibler (2012). "Effect of body position on ventilation distribution in preterm infants on continuous positive airway pressure." Pediatric Critical Care Medicine **13**(4): 446-451.

Hough, J. L., T. M. T. Pham and A. Schibler (2014). "Physiologic effect of high-flow nasal cannula in infants with bronchiolitis." Pediatric Critical Care Medicine **15**(5): e214-219.

Humphreys, S., T. M. Pham, C. Stocker and A. Schibler (2011). "The effect of induction of anesthesia and intubation on end-expiratory lung level and regional ventilation distribution in cardiac children." Paediatric Anaesthesia **21**(8): 887-893.

Hutchings, F. A., T. N. Hilliard and P. J. Davis (2015). "Heated humidified high-flow nasal cannula therapy in children." Archives Of Disease In Childhood **100**(6): 571-575.

Itagaki, T., N. Okuda, Y. Tsunano, H. Kohata, E. Nakataki, M. Onodera, H. Imanaka and M. Nishimura (2014). "Effect of High-Flow Nasal Cannula on Thoraco-Abdominal Synchrony in Adult Critically Ill Patients." Respiratory Care **59**(1): 70-74.

Jones, A. Y., E. Dean and C. C. Chow (2003). "Comparison of the oxygen cost of breathing exercises and spontaneous breathing in patients with stable chronic obstructive pulmonary disease." Physical Therapy **83**(5): 424-431.

Kallet, R. H., A. R. Campbell, J. A. Alonso, D. J. Morabito and R. C. Mackersie (2000). "The effects of pressure control versus volume control assisted ventilation on patient work of breathing in acute lung injury and acute respiratory distress syndrome." Respiratory Care **45**(9): 1085-1096.

Kallio, M., O. Peltoniemi, E. Anttila, T. Pokka and T. Kontiokari (2015). "Neurally adjusted ventilatory assist (NAVA) in pediatric intensive care--a randomized controlled trial." Pediatric Pulmonology **50**(1): 55-62.

Klein, M. and L. Reynolds (1986). "Relief of sleep-related oropharyngeal airway obstruction by continuous insufflation of the pharynx." The Lancet **327**(8487): 935-939.

Kotecha, S. J., R. Adappa, N. Gupta, W. J. Watkins, S. Kotecha and M. Chakraborty (2015). "Safety and Efficacy of High-Flow Nasal Cannula Therapy in Preterm Infants: A Meta-analysis." Pediatrics **136**(3): 542-553.

Kubicka, Z. J., J. Limauro and R. A. Darnall (2008). "Heated, humidified high-flow nasal cannula therapy: yet another way to deliver continuous positive airway pressure?" Pediatrics **121**(1): 82-88.

Lampland, A. L., B. Plumm, P. A. Meyers, C. T. Worwa and M. C. Mammel (2009). "Observational study of humidified high-flow nasal cannula compared with nasal continuous positive airway pressure." The Journal of Pediatrics **154**(2): 177-182.

Larouche, A., E. Massicotte, G. Constantin, L. Ducharme-Crevier, S. Essouri, C. Sinderby, J. Beck and G. Emeriaud (2015). "Tonic diaphragmatic activity in critically ill children with and without ventilatory support." Pediatric Pulmonology **50**(12): 1304-1312.

Lavizzari, A., C. Veneroni, M. Colnaghi, F. Ciuffini, E. Zannin, M. Fumagalli, F. Mosca and R. L. Dellacà (2014). "Respiratory mechanics during NCPAP and HHHFNC at equal distending pressures." Archives Of Disease In Childhood. Fetal And Neonatal Edition **99**(4): F315-320.

Lee, J. H., K. J. Rehder, L. Williford, I. M. Cheifetz and D. A. Turner (2013). "Use of high flow nasal cannula in critically ill infants, children, and adults: a critical review of the literature." Intensive Care Medicine **39**(2): 247-257.

Liet, J.-M., J.-M. Dejode, N. Joram, B. Gaillard-Le Roux, P. Bétrémieux and J.-C. Rozé (2011). "Respiratory support by neurally adjusted ventilatory assist (NAVA) in severe RSV-related bronchiolitis: a case series report." BMC Pediatrics **11**: 92.

Long, E., F. E. Babl and T. Duke (2016). "Is there a role for humidified heated high-flow nasal cannula therapy in paediatric emergency departments?" Emergency Medicine Journal: [Epub ahead of print].

Lopes, J., N. L. Muller, M. H. Bryan and A. C. Bryan (1981). "Importance of inspiratory muscle tone in maintenance of FRC in the newborn." Journal of Applied Physiology Respiratory Environmental and Exercise Physiology **51**(4): 830-834.

Manley, B. J., S. K. Dold, P. G. Davis and C. C. Roehr (2012). "High-flow nasal cannulae for respiratory support of preterm infants: a review of the evidence." Neonatology **102**(4): 300-308.

Mayfield, S., J. Jauncey-Cooke and F. Bogossian (2013). "A case series of paediatric high flow nasal cannula therapy." Australian Critical Care **26**(4): 189-192.

Mayfield, S., J. Jauncey-Cooke, J. L. Hough, A. Schibler, K. Gibbons and F. Bogossian (2014). "High-flow nasal cannula therapy for respiratory support in children." The Cochrane Database Of Systematic Reviews **3**: CD009850.

McKiernan, C., L. C. Chua, P. F. Visintainer and H. Allen (2010). "High Flow Nasal Cannulae Therapy in Infants with Bronchiolitis." The Journal of Pediatrics **156**(4): 634-638.

McQueen, M., J. Rojas, S. C. Sun, R. Tero, K. Ives, F. Bednarek, L. Owens, K. Dysart, G. Dungan, T. H. Shaffer and T. L. Miller (2014). "Safety and Long Term Outcomes with

High Flow Nasal Cannula Therapy in Neonatology: A Large Retrospective Cohort Study." Journal Of Pulmonary & Respiratory Medicine **4**(6): 216.

Milési, C., M. Boubal, A. Jacquot, J. Baleine, S. Durand, M. P. Odena and G. Cambonie (2014). "High-flow nasal cannula: recommendations for daily practice in pediatrics." Annals Of Intensive Care **4**: 29.

Mundel, T., S. Feng, S. Tatkov and H. Schneider (2013). "Mechanisms of nasal high flow on ventilation during wakefulness and sleep." Journal Of Applied Physiology **114**(8): 1058-1065.

Nishimura, M. (2015). "High-flow nasal cannula oxygen therapy in adults." Journal Of Intensive Care **3**(1): 15.

Pandit, P. B., S. E. Courtney, K. H. Pyon, J. G. Saslow and R. H. Habib (2001). "Work of Breathing During Constant- and Variable-Flow Nasal Continuous Positive Airway Pressure in Preterm Neonates." Pediatrics **108**(3): 682-685.

Parke, R., S. McGuinness and M. Eccleston (2009). "Nasal high-flow therapy delivers low level positive airway pressure." British Journal of Anaesthesia **103**(6): 886-890.

Pham, T. M., M. Yuill, C. Dakin and A. Schibler (2011). "Regional ventilation distribution in the first 6 months of life." The European Respiratory Journal **37**(4): 919-924.

Pham, T. M. T., L. O'Malley, S. Mayfield, S. Martin and A. Schibler (2015). "The effect of high flow nasal cannula therapy on the work of breathing in infants with bronchiolitis." Pediatric Pulmonology **50**(7): 713-720.

Prisk, G. K., J. Hammer and C. J. L. Newth (2002). "Techniques for measurement of thoracoabdominal asynchrony." Pediatric Pulmonology **34**(6): 462-472.

Ralston, S. L., A. S. Lieberthal, H. C. Meissner, B. K. Alverson, J. E. Baley, A. M. Gadomski, D. W. Johnson, M. J. Light, N. F. Maraqa, E. A. Mendonca, K. J. Phelan, J. J. Zorc, D. Stanko-Lopp, M. A. Brown, I. Nathanson, E. Rosenblum, S. Sayles, 3rd and S. Hernandez-Cancio (2014). "Clinical practice guideline: the diagnosis, management, and prevention of bronchiolitis." Pediatrics **134**(5): e1474-1502.

Ravaglia, C. and V. Poletti (2014). "Recent advances in the management of acute bronchiolitis." F1000prime Reports **6**: 103.

Reiterer, F., E. Sivieri and S. Abbasi (2015). "Evaluation of bedside pulmonary function in the neonate: From the past to the future." Pediatric Pulmonology **50**(10): 1039-1050.

Riese, J., J. Fierce, A. Riese and B. K. Alverson (2015). "Effect of a Hospital-wide High-Flow Nasal Cannula Protocol on Clinical Outcomes and Resource Utilization of Bronchiolitis Patients Admitted to the PICU." Hospital Pediatrics **5**(12): 613-618.

Rödl, S., B. Resch, N. Hofer, I. Marschitz, G. Madler, E. Eber and G. Zobel (2012). "Prospective evaluation of clinical scoring systems in infants with bronchiolitis admitted to the intensive care unit." European Journal of Clinical Microbiology & Infectious Diseases **31**(10): 2667-2672.

Rubin, S., A. Ghuman, T. Deakers, R. Khemani, P. Ross and C. J. Newth (2014). "Effort of breathing in children receiving high-flow nasal cannula." Pediatric Critical Care Medicine **15**(1): 1-6.

Saslow, J. G., Z. H. Aghai, T. A. Nakhla, J. J. Hart, R. Lawrysh, G. E. Stahl and K. H. Pyon (2006). "Work of breathing using high-flow nasal cannula in preterm infants." Journal Of Perinatology **26**(8): 476-480.

Sassoon, C. S., R. W. Light, R. Lodia, G. C. Sieck and C. K. Mahutte (1991). "Pressure-time product during continuous positive airway pressure, pressure support ventilation, and T-piece during weaning from mechanical ventilation." The American Review Of Respiratory Disease **143**(3): 469-475.

Schibler, A., T. M. Pham, A. A. Moray and C. Stocker (2013). "Ventilation and cardiac related impedance changes in children undergoing corrective open heart surgery." Physiological Measurement **34**(10): 1319-1327.

Schibler, A., T. M. T. Pham, K. R. Dunster, K. Foster, A. Barlow, K. Gibbons and J. L. Hough (2011). "Reduced intubation rates for infants after introduction of high-flow nasal prong oxygen delivery." Intensive Care Medicine **37**(5): 847-852.

Schibler, A., M. Yuill, C. Parsley, T. Pham, K. Gilshenan and C. Dakin (2009). "Regional ventilation distribution in non-sedated spontaneously breathing newborns and adults is not different." Pediatric Pulmonology **44**(9): 851-858.

Sinderby, C. and J. Beck (2013). "Neurally adjusted ventilatory assist in non-invasive ventilation." Minerva Anestesiologica **79**(8): 915-925.

Sinderby, C., J. Beck, J. Spahija, J. Weinberg and A. Grassino (1998). "Voluntary activation of the human diaphragm in health and disease." Journal Of Applied Physiology **85**(6): 2146-2158.

Sinha, I. P., A. K. S. McBride, R. Smith and R. M. Fernandes (2015). "CPAP and High-Flow Nasal Cannula Oxygen in Bronchiolitis." Chest **148**(3): 810-823.

Sotello, D., M. Orellana-Barrios, A. M. Rivas and K. Nugent (2015). "High Flow Nasal Cannulas for Oxygenation: An Audit of Its Use in a Tertiary Care Hospital." The American Journal Of The Medical Sciences **350**(4): 308-312.

Spoletini, G., M. Alotaibi, F. Blasi and N. S. Hill (2015). "Heated Humidified High-Flow Nasal Oxygen in Adults: Mechanisms of Action and Clinical Implications." Chest **148**(1): 253-261.

Suarez-Sipmann, F. (2014). "New modes of assisted mechanical ventilation." Medicina Intensiva **38**(4): 249-260.

ten Brink, F., T. Duke and J. Evans (2013). "High-flow nasal prong oxygen therapy or nasopharyngeal continuous positive airway pressure for children with moderate-to-severe respiratory distress?*." Pediatric Critical Care Medicine **14**(7): e326-331.

Terzi, N. and P. Navalesi (2014). "Inspiratory muscle activity in neurally adjusted ventilatory assist: more than sonata for "solo diaphragm"." Anesthesiology **121**(5): 916-918.

Urbano, J., J. del Castillo, J. Lopez-Herce, J. A. Gallardo, M. J. Solana and A. Carrillo (2012). "High-flow oxygen therapy: pressure analysis in a pediatric airway model." Respiratory Care **57**(5): 721-726.

Vagheggini, G., S. Mazzoleni, E. Vlad Panait, P. Navalesi and N. Ambrosino (2013). "Physiologic response to various levels of pressure support and NAVA in prolonged weaning." Respiratory Medicine **107**(11): 1748-1754.

Vassilakopoulos, T. and B. J. Petrof (2004). "Ventilator-induced diaphragmatic dysfunction." American Journal Of Respiratory And Critical Care Medicine **169**(3): 336-341.

Ververidis, D., M. Van Gils, C. Passath, J. Takala and L. Brander (2011). "Identification of Adequate Neurally Adjusted Ventilatory Assist (NAVA) During Systematic Increases in the NAVA Level." IEEE Transactions on Biomedical Engineering **58**(9): 2598-2606.

Wilkinson, D., C. Andersen, C. P. O'Donnell, A. G. De Paoli and B. J. Manley (2016). "High flow nasal cannula for respiratory support in preterm infants." The Cochrane Database Of Systematic Reviews **2**(22): CD006405.

Wolf, G. K., B. K. Walsh, M. L. Green and J. H. Arnold (2011). "Electrical activity of the diaphragm during extubation readiness testing in critically ill children." Pediatric Critical Care Medicine **12**(6): e220-224.